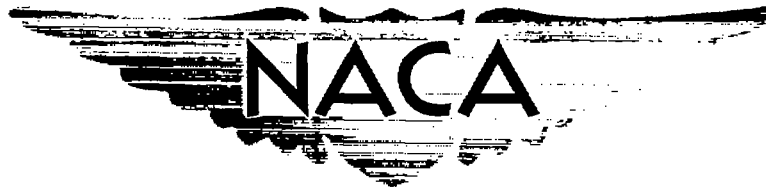


NACA RM E9109



RESEARCH MEMORANDUM

COOLING OF RAM JETS AND TAIL-PIPE BURNERS - ANALYTICAL
METHOD FOR DETERMINING TEMPERATURES OF COMBUSTION
CHAMBER HAVING ANNULAR COOLING PASSAGE

By William K. Koffel, Eugene Stamper
and Newell D. Sanders

Lewis Flight Propulsion Laboratory
Cleveland, Ohio

CLASSIFIED DOCUMENT

This document contains classified information affecting the National Defense of the United States within the meaning of the Espionage Act, USC 5031 and 32. Its transmission or the revelation of its contents in any manner to an unauthorized person is prohibited by law. Information so classified may be imparted only to persons in the military and naval services of the United States, appropriate civilian officers and employees of the Federal Government who have a legitimate interest therein, and to United States citizens of known loyalty and discretion who of necessity must be informed thereof.

NATIONAL ADVISORY COMMITTEE FOR AERONAUTICS

WASHINGTON
March 21, 1950



NATIONAL ADVISORY COMMITTEE FOR AERONAUTICS


RESEARCH MEMORANDUMCOOLING OF RAM JETS AND TAIL-PIPE BURNERS - ANALYTICAL
METHOD FOR DETERMINING TEMPERATURES OF COMBUSTION
CHAMBER HAVING ANNULAR COOLING PASSAGEBy William K. Koffel, Eugene Stamper
and Newell D. Sanders

SUMMARY

An analytical method is given for calculating the maximum wall temperature of a tail-pipe burner or a ram-jet combustion chamber cooled by air or gas flowing through a surrounding annular passage. Data from step-by-step integrations of the heat flow from the combustion gas to the cooling gas, which take into consideration the longitudinal temperature distribution of the combustion gases, the variation of heat-transfer coefficients along the burner length, and radiation from combustion gases to the combustion-chamber wall, are used to develop an empirical equation expressing the outlet temperature of the cooling gas in terms of known conditions of flow and geometry. When the outlet cooling-gas temperature is known, two parameters can be evaluated that make possible the determination of the maximum temperature of the inside wall from a working chart, which is a solution of the heat balance across the inside wall at the outlet.

Extensive combinations and ranges of the independent variables (mass velocity of combustion gas, mass velocity of cooling gas, inlet cooling-air temperature, final combustion-gas temperature, burner diameter, cooling-passage height, burner length, and fins) have been generalized by the empirical equation, which greatly reduces the labor of calculating the inside-wall temperature.

Temperatures calculated by this method show satisfactory agreement with corresponding temperatures measured on several experimental tail-pipe burners. Corresponding temperatures calculated at a station 0.7 of the distance from the flame holder to the nozzle outlet are within $\pm 15^\circ$ of the measured cooling-gas temperature and within approximately $\pm 25^\circ$ of the measured inside-wall temperature.



The difference between the measured and calculated inside-wall temperatures ranges from about 0.06 to 0.16 of the difference between the measured temperatures of the inside wall and the cooling gas.

INTRODUCTION

Installations of tail-pipe burners for augmenting thrust at take-off, in combat emergencies, and for acceleration through the transonic region urgently demand the solution of cooling problems inherent in such installations. The combustion temperatures in tail-pipe burners and in ram jets reach 3000° to 4000° R. The durability of high-temperature alloys currently used in construction of tail-pipe burners and ram-jet combustion chambers is impaired by operating temperatures greater than about 2000° R (reference 1). For continuous operation, some means must be provided to prevent overheating of the burner wall and to protect the aircraft structure and accessories from high temperatures.

Some suggested methods for maintaining burner-wall temperatures within safe limits make use of stratification of combustion to provide cool air or gases between the wall and the hot gases (reference 2), a liquid-cooling jacket (reference 3), a regenerative fuel preheater jacket (reference 4), a ceramic combustion-chamber lining (reference 5), a thin wall cooled by convection and radiation to the free stream (reference 6), and air flowing through an annular cooling passage surrounding the combustion chamber (references 2 and 7). Cooling of exhaust pipes and tail pipes in which there is no combustion is discussed in reference 7.

Several of these cooling systems are being experimentally and analytically investigated at the NACA Lewis laboratory. Cooling by means of an annular air passage is being intensively investigated. Results of a detailed investigation on cooling of tail-pipe burners and ram-jet combustion chambers are presented herein. The analysis is primarily concerned with heat transfer and temperatures and does not consider the pressure losses through the cooling passage or the effect of the cooling system on over-all performance.

Calculation of the maximum inside-wall temperature from a heat balance across the wall at the outlet requires the solution of a fourth-degree algebraic equation. This equation is converted into a nondimensional form and presented as a working chart in which the inside-wall temperature is given in terms of two parameters involving known temperatures, mass flows, geometry, and materials.

The cooling-gas temperature at the outlet of the cooling passage is not generally known, but it is a function of the heat received from the inside wall and the heat given up to the outside wall. The analysis presented herein develops an empirical method for obtaining the cooling-gas temperature at the outlet as an aid in determining the maximum inside-wall temperature. Calculated data from a number of tedious step-by-step solutions of the heat balance across the inside wall are generalized in an empirical equation that relates the outlet cooling-gas temperature to mass velocity of cooling gas, mass velocity of combustion gas, inlet cooling-gas temperature, outlet combustion-gas temperature, burner diameter, cooling-passage height, and burner length. The approximate range of variables investigated in the development of the empirical equation are summarized in the following table:

| | |
|---|-------------|
| Burner diameter, in. | 10-40 |
| Cooling-passage height, in. | 1/8-7/8 |
| Burner length, ft | 4-10 |
| Mass velocity of combustion gas, lb/(sec)(sq ft) | 3.9-32 |
| Mass velocity of cooling gas, lb/(sec)(sq ft) | 1.5-51 |
| Mass ratio, cooling gas to combustion gas | 0.015-0.33 |
| Total pressure upstream of flame holder, lb/sq ft absolute | 550-6000 |
| Inlet total temperature of cooling gas, °R | 400-1700 |
| Inlet total temperature of combustion gas, °R | 400-1700 |
| Outlet total temperature of combustion gas, °R | 2000-3700 |
| Longitudinal fins: | |
| Thickness, in. | 1/16 |
| Spacing, in. | 1/2 |
| Height, in. | 1/4 and 1/2 |

An example problem included in appendix A illustrates the use of the empirical equation and the determination of the maximum inside-wall temperature from the chart.

CONFIGURATION AND ASSUMPTIONS

Configuration

An annular cooling passage formed by a concentric liner inside a tail-pipe burner or a ram-jet combustion chamber is shown in figure 1(a). Part of the diffuser mass flow is diverted through the annular passage for cooling purposes. Unless otherwise stated, the succeeding discussion refers to a tail-pipe burner with part of the

turbine-outlet gas used for cooling, but the method of analysis applies equally well to a ram jet cooled with air or to a tail-pipe burner cooled with air flowing through an external shroud.

Basic Assumptions

The following basic assumptions were made in calculating the data used to develop the empirical equation relating the outlet cooling-gas temperature to the independent design and operating variables:

1. Steady-state conditions
2. Flow passages of constant cross-sectional area
3. One-dimensional flow
4. Linear combustion-temperature rise from inlet to outlet
5. Fully developed turbulent flow
6. Twice nonluminous radiation from combustion gas to inside wall
7. Negligible temperature drop across inside wall and no longitudinal conduction
8. No heat flow through outside wall

Discussion of Assumptions

One-dimensional flow. - The assumption of one-dimensional flow is permissible in the cooling passage where transverse temperature gradients are not large. Large transverse temperature gradients are created in the combustion gas by the combustion pattern, which is largely influenced by the flame-holder design and radial clearance with the inside wall and by the manner of fuel injection. A uniform transverse temperature distribution is assumed in the absence of experimental data relating the combustion-gas temperature at the wall to the integrated mean combustion-gas temperature. This assumption is conservative because, in the usual case, the gas temperature at the wall is lower than the mean gas temperature; however, if flames should impinge directly on the inside wall, this assumption should still be valid.

1227

Linear combustion-temperature rise. - Typical longitudinal distribution of the mean combustion-gas temperature is shown in figure 2. The data were calculated from measured static-pressure distributions on two 20-inch-diameter ram-jet combustion chambers of different length. A small simplification of this analysis is achieved by assuming a linear rise in combustion temperature with length. Trial calculations using step-by-step integration to check the effect of several assumed distributions of combustion-gas temperature (fig. 3) show some effect on the outlet cooling-gas temperature and an even smaller effect on the maximum inside-wall temperature.

Fully developed turbulent flow. - The equivalent of fully developed turbulent flow is considered to exist at the inlet of the cooling passage and at the inlet of the combustion chamber although actual flow conditions may be different.

Radiation from combustion gas to inside wall. - Radiation from the combustion gas to the inside wall is difficult to estimate because of the unknown degree of luminosity of the combustion flames and because of inadequate data on the emissivity and absorptivity of luminous flames. Reference 8 states that radiation from soot in industrial furnaces is of a greater order of magnitude than nonluminous radiation. Luminous acetylene flames are reported (reference 9) to radiate roughly four times as much as when nonluminous. The high combustion efficiency of a burner results in comparatively fewer luminous particles than in a sooty flame and the radiant heat from the combustion gas is therefore probably between the nonluminous value and four times the nonluminous value. The calculated data used in developing the empirical equation in this report are based on the estimate of twice the nonluminous radiation as given in reference 8. The mass ratios of carbon dioxide and of water vapor to combustion-gas products were assumed to be the same as those corresponding to complete combustion of a stoichiometric mixture of air and $C_{12}H_{26}$ (same molecular weight as kerosene).

Negligible temperature drop and no longitudinal conduction. - The inside wall is assumed thin enough that the temperature drop across the wall is negligible, and the thermal conductivity and longitudinal temperature gradients in the wall are small enough to eliminate consideration of longitudinal flow of heat.

No heat flow through outside wall. - The assumption of no heat flow through the outside wall eliminates an additional heat

balance and greatly simplifies the calculations. The outside-wall temperature was therefore assumed as equal to the local cooling-air temperature. This assumption is satisfactory in cases where the outside wall is insulated from the surroundings and gives a conservative estimate of cooling requirements in cases where there is external heat loss. When the heat flow through the outside wall is appreciable, the method used for calculating the outlet cooling-gas temperature without heat losses can be applied and then corrected for heat losses through the outside wall.

SYMBOLS

The following symbols are used in this report:

| | |
|------------------------|---|
| A | area normal to flow direction, (sq ft) |
| a, d, j, m, u, v, z | exponents |
| B | $\frac{W_c c_{p,c}}{U \pi D_1}$ |
| b | cooling-passage height, $\frac{D_o - D_1}{2}$, (ft) |
| C | exposed perimeter, (ft) |
| c_p | specific heat at constant pressure, (Btu/(lb)(°R)) |
| D_h | hydraulic diameter, (ft) |
| D_1 | outside diameter of inside wall or burner diameter, (ft) |
| D_o | inside diameter of outside wall, (ft) |
| $F_{A,E}$ | modulus that modifies equation for radiation between black bodies to account for emissivities and relative geometries |
| G | mass velocity, (lb/(sec)(sq ft)) |
| h | heat-transfer coefficient, (Btu/(hr)(sq ft)(°R)) |
| K | factor in equation (19) |
| k | thermal conductivity, (Btu/(hr)(sq ft)(°R/ft)) |

| | |
|---------------|---|
| L | beam length, (ft)(reference 8, p. 69) |
| l | length or height, (ft) |
| n | number of fins |
| P | total pressure, (lb/sq ft absolute) |
| p | static pressure, (lb/sq ft absolute) |
| q | heat flow, (Btu/hr) |
| S | surface area, (sq ft) |
| s | distance between surfaces of adjacent fins, (ft) |
| T | total temperature, ($^{\circ}\text{R}$) |
| T_m | arithmetic average of surface temperature and free-air temperature, ($^{\circ}\text{R}$) |
| t | static or surface temperature, ($^{\circ}\text{R}$) |
| U | effective over-all heat-transfer coefficient |
| V_0 | velocity of undisturbed air stream, (ft/sec) |
| W | mass flow, (lb/sec) |
| x | distance, (ft) |
| y | thickness, (ft) |
| α | absorptivity |
| β | constant of proportionality |
| ρ | density of air at temperature T_m and prevalent pressure, (lb/cu ft) |
| ϵ | emissivity |
| ϵ'_w | pseudoemissivity of wall |
| σ | Stefan-Boltzmann constant, 0.173×10^{-8} (Btu/(sq ft)(hr)($^{\circ}\text{R}^4$)) |

Parameters:

$$\varphi = \frac{\psi^3_{CO_2}(F_{A,E} + \epsilon'_w \alpha_g)}{h_g + h_c \left(1 - \frac{ny_f}{\pi D_1}\right) + \frac{n}{\pi D_1} \sqrt{h_c C k_f y_f} \tanh l_f \sqrt{\frac{h_c C}{k_f y_f}}}$$

$$\psi = \frac{T_g^4 \epsilon'_w \epsilon_g + T_g h_g + T_c^4 \alpha_{F_{A,E}} + T_c \left[h_c \left(1 - \frac{ny_f}{\pi D_1}\right) + \frac{n}{\pi D_1} \sqrt{h_c C k_f y_f} \tanh l_f \sqrt{\frac{h_c C}{k_f y_f}} \right]}{h_g + h_c \left(1 - \frac{ny_f}{\pi D_1}\right) + \frac{n}{\pi D_1} \sqrt{h_c C k_f y_f} \tanh l_f \sqrt{\frac{h_c C}{k_f y_f}}}$$

Subscripts:

- av average
- CO₂ carbon dioxide in combustion gas
- c cooling gas or cooling passage
- d diffuser outlet
- f fin
- g combustion gas or combustion chamber
- H₂O water vapor in combustion gas
- i inside wall
- o outside wall
- r radiation
- w wall
- x variable station
- 0 ambient or surrounding
- 1 inlet station or preceding station (fig. 1)
- 2 outlet station or succeeding station (fig. 1)

HEAT BALANCE AND DETERMINATION OF WALL TEMPERATURE

Under equilibrium conditions, the heat transfer from the combustion gas to the inside wall is balanced by the heat lost to the cooling air, and the equilibrium temperature of the wall can be obtained from the heat-balance equation in terms of known temperatures, heat-transfer coefficients, emissivities, and geometry. Inasmuch as the heat balance is a fourth-degree algebraic equation, a chart is developed that reduces the labor of calculating the inside-wall temperature.

Heat-Transfer Equations

Convective heat transfer. - Convective heat transfer between a gas and a surface is given by Newton's law of cooling

$$\frac{q}{S} = h(T_g - t_w) \quad (1)$$

where h depends on the fluid flow conditions. The convective heat-transfer coefficient h for turbulent flow of air in long ducts may be obtained from reference 10 as

$$h = 0.378 \frac{T^{0.3} G^{0.8}}{D_h^{0.2}} \quad (2)$$

Equation (2) is used to estimate convective heat-transfer coefficients in the combustion chamber and the cooling passage.

For circular ducts, the hydraulic diameter D_h is equal to the geometrical diameter. The hydraulic diameter of a noncircular duct is four times the flow area divided by the wetted perimeter. In the case of an annulus, the hydraulic diameter is

$$D_h = D_o - D_i \quad (3)$$

and for a rectangular fin passage

$$D_h = \frac{2sl_f}{s+l_f} \quad (4)$$

where l_f is the fin height and s is the distance between surfaces of adjacent fins.

Radiant heat transfer from combustion gas. - The radiant heat transferred from the combustion gas to the inside wall is given (reference 8) by the equation

$$\frac{q_{r,g}}{S} = \sigma \epsilon'_w (\epsilon_g T_g^4 - \alpha_g t_1^4) \quad (5)$$

where

$$\epsilon'_w = \frac{\epsilon_w + 1}{2} \quad (6)$$

and ϵ_g and α_g are evaluated from charts in reference 8. Emissivities of surfaces are given in references 8 and 11.

Radiant heat transfer between walls of cooling passage. - If the outside-wall temperature is assumed equal to the local cooling-gas temperature, the radiant heat transfer between the walls of the cooling passage is expressed by

$$\frac{q_{r,w}}{S} = \sigma F_{A,E} (t_1^4 - T_c^4) \quad (7)$$

where $F_{A,E}$ is a combined shape-emissivity modulus that modifies the equation for radiation between black bodies to account for the emissivities and the relative geometries of the radiating surfaces. Reference 10 gives $F_{A,E}$ for infinite concentric cylinders as

$$F_{A,E} = \frac{1}{\frac{1}{\epsilon_1} + \frac{S_1}{S_0} \left(\frac{1}{\epsilon_0} - 1 \right)} \quad (8)$$

which is sufficiently accurate for the annular cooling passage with or without longitudinal fins in the passage.

Heat transfer to fins. - The heat transfer from a finite bar fin (Fig. 1(b)) of constant cross-sectional area with no heat flow through the end of the fin tip is given in reference 12 as

$$q_f = \sqrt{h_o C k_f A_f} (t_1 - T_c) \tanh l_f \sqrt{\frac{h_o C}{k_f A_f}} \quad (9)$$

where

$$A_f = y_f \text{ per unit of length}$$

Use of equation (9) in this analysis is limited to cases where fins are spaced close enough to maintain an essentially constant wall temperature between fin bases.

Heat Balance

The balance of heat received and given up by the inside wall is

$$q_{r,g} + q_g = q_{r,w} + q_c + nq_f \quad (10)$$

Substitution of equations (1), (5), (7), and (9) into equation (10) and representing S per unit of length gives

$$\begin{aligned} & \sigma \epsilon'_w (\epsilon_g T_g^4 - \alpha_g t_1^4) \pi D_1 + h_g (T_g - t_1) \pi D_1 \\ & = \sigma F_{A,E} (t_1^4 - T_c^4) \pi D_1 + h_c (t_1 - T_c) (\pi D_1 - n y_f) + n \sqrt{h_c C k_f y_f} (t_1 - T_c) \tanh l_f \sqrt{\frac{h_c C}{k_f y_f}} \end{aligned} \quad (11)$$

Dividing equation (11) by πD_1 and expanding and collecting like terms give

$$\begin{aligned} & t_1^4 \sigma (F_{A,E} + \epsilon'_w \alpha_g) + t_1 \left[h_g + h_c \left(1 - \frac{n y_f}{\pi D_1} \right) + \frac{n}{\pi D_1} \sqrt{h_c C k_f y_f} \tanh l_f \sqrt{\frac{h_c C}{k_f y_f}} \right] \\ & = T_g^4 \sigma \epsilon'_w \epsilon_g + T_g h_g + T_c^4 \sigma F_{A,E} + T_c \left[h_c \left(1 - \frac{n y_f}{\pi D_1} \right) + \frac{n}{\pi D_1} \sqrt{h_c C k_f y_f} \tanh l_f \sqrt{\frac{h_c C}{k_f y_f}} \right] \end{aligned} \quad (12)$$

Determination of Inside-Wall Temperature

The unknown inside-wall temperature t_1 is related in equation (12) to the known temperatures, mass flows, geometry, and materials. Rearranging equation (12) gives

$$\varphi \left(\frac{t_1}{\psi} \right)^4 + \frac{t_1}{\psi} = 1 \quad (13)$$

where

$$\psi = \frac{T_g^4 \sigma \epsilon'_w \epsilon_g + T_g h_g + T_c^4 \sigma F_{A,E} + T_c \left[h_c \left(1 - \frac{n y_f}{\pi D_1} \right) + \frac{n}{\pi D_1} \sqrt{h_c C k_f y_f} \tanh l_f \sqrt{\frac{h_c C}{k_f y_f}} \right]}{h_g + h_c \left(1 - \frac{n y_f}{\pi D_1} \right) + \frac{n}{\pi D_1} \sqrt{h_c C k_f y_f} \tanh l_f \sqrt{\frac{h_c C}{k_f y_f}}} \quad (14)$$

and

$$\varphi = \frac{\psi^3 \sigma (F_{A,E} + \epsilon'_w \alpha_g)}{h_g + h_c \left(1 - \frac{n y_f}{\pi D_1} \right) + \frac{n}{\pi D_1} \sqrt{h_c C k_f y_f} \tanh l_f \sqrt{\frac{h_c C}{k_f y_f}}} \quad (15)$$

With no fins in the cooling passage, n is zero and the parameters ψ and φ reduce to

$$\psi = \frac{T_g^4 \sigma \epsilon'_w \epsilon_g + T_g h_g + T_c^4 \sigma F_{A,E} + T_c h_c}{h_g + h_c} \quad (16)$$

$$\varphi = \frac{\psi^3 \sigma (F_{A,E} + \epsilon'_w \alpha_g)}{h_g + h_c} \quad (17)$$

The temperature of the inside wall can now be read from a plot (fig. 4) of equation (13) when the parameters φ and ψ are evaluated. It is noted that φ contains α_g , which depends on the value of t_1 and must therefore be estimated. At a wall temperature of 1960° R, the average rate of decrease of α_g with t_1

is about 10 percent per 100° increase in t_1 and, because the contribution of $\epsilon'w\alpha_g$ to ϕ is small, a second estimate of α_g is generally unnecessary. The outlet temperature of the cooling gas that appears in the parameter ψ is obtained from an empirical equation developed in the following section.

EMPIRICAL EQUATION FOR COOLING-GAS TEMPERATURE

Direct solution of the differential equation relating the outlet cooling-gas temperature to the independent variables, passage height b , passage length l , burner diameter D_1 , mass velocity of combustion gas G_g , mass velocity of cooling gas G_c , combustion-gas temperature distribution, and inlet cooling-gas temperature, is impossible because the heat-transfer coefficients vary with temperature along the length of the burner. The differential equation for the temperatures in the cooling passage can be solved when the simplifying assumptions of constant heat-transfer coefficients and constant gas properties are made. Solution of the differential equation using these simplifications gives the characteristic equation

$$\frac{T_{g,2} - T_{c,2}}{T_{g,2} - T_{g,1}} = \frac{1 - \left[1 - \frac{T_{g,1} - T_{c,1}}{T_{g,2} - T_{g,1}} \left(\frac{lU}{bG_c c_{p,c}} \right) \right] e^{-\frac{lU}{bG_c c_{p,c}}}}{\frac{lU}{bG_c c_{p,c}}} \quad (18)$$

which is derived in appendix B and plotted in figure 5 for given values of the dimensionless parameters $\frac{T_{g,1} - T_{c,1}}{T_{g,2} - T_{g,1}}$ and $\frac{lU}{bG_c c_{p,c}}$.

Fitting Empirical Equation

The succeeding paragraphs develop an empirical equation, which evaluates the parameter $\frac{lU}{bG_c c_{p,c}}$ from the results of a number of step-by-step solutions for the outlet cooling-gas temperature. The data obtained from the step-by-step solutions are presented in table I.

The unknown quantity in the parameter $\frac{bG_c c_{p,c}}{2U}$ is the effective over-all heat-transfer coefficient U . The value of U is related to Reynolds number of the cooling-gas flow, the Reynolds number of the combustion-gas flow, and the temperature of cooling gas and combustion gas. Because of this relation, the parameter $\frac{bG_c c_{p,c}}{2U}$ is related to the independent variables by the following approximate empirical equation:

$$\frac{bG_c c_{p,c}}{2U} = K \left(\frac{G_c}{G_g} \right)^a G_g^d D_1^j b_m^m U_{T_g,2}^v T_{c,1}^z \quad (19)$$

The constants in this equation can be adjusted to fit the results of the step-by-step solutions that take into consideration the variation in heat-transfer coefficient. This fitting is accomplished by selecting the proper values for the factor K and the seven exponents a , d , j , m , u , v , and z .

The method of selecting the values of the exponents is illustrated by the selection of a . From the results of the step-by-step calculations (table I), in which G_c/G_g was varied and all other quantities held constant, values of $\frac{T_{g,2}-T_{c,2}}{T_{g,2}-T_{g,1}}$ are obtained. The corresponding values of $\frac{T_{g,1}-T_{c,1}}{T_{g,2}-T_{g,1}}$ are found from the initial

conditions. The values of $\frac{bG_c c_{p,c}}{2U}$ obtained from figure 5 are then plotted against G_c/G_g on logarithmic coordinates, as shown in figure 6(a). The data fall in straight lines and each line represents a constant set of operating conditions and geometry. The slope of each line is the exponent a . The value of a in equation (19) is assumed to be independent of the variables; this assumption is shown to be approximately correct by the fact that lines representing widely different conditions are practically parallel.

A similar procedure is employed in determining the values of the other exponents (figs. 6(b) to 6(g)). The extent to which the value of each exponent is independent of the values of the other variables can be seen by the approach to parallelism in figures 6(b) to 6(g). The values of the exponents thus determined are as follows:

$$a = 0.84$$

$$d = 0.29$$

$$j = 0$$

$$m = 1.2$$

$$u = -1.0$$

$$v = -0.38$$

$$z = -0.23$$

The values of the variables from the step-by-step solutions and the corresponding values of $\frac{bG_c c_{p,c}}{2U}$ from figure 5 are substituted into equation (19) along with the tabulated values for the exponents, to determine the factor K. The mean value of K (fig. 7) is 50,000 with a spread of ± 0.14 from the mean value, which is an indication of the over-all accuracy of the empirical equation in correlating the range of combinations investigated in the step-by-step calculations.

In a ram jet having an outlet combustion-gas temperature of 3500°R , a combustion-chamber-inlet temperature of 500°R , and an inlet cooling-air temperature of 500°R , an uncertainty of ± 0.14 in K causes variations in cooling-air temperature rise from the mean temperature rise of the cooling air of about ± 0.15 and ± 0.03 at $\frac{bG_c c_{p,c}}{2U}$ equal to 1.5 and 5, respectively. In these regions the effect of outlet cooling-air temperature on the maximum inside-wall temperature is approximately 1° change in wall temperature per 10° change in cooling-air temperature for $\frac{bG_c c_{p,c}}{2U}$ of 1.5 and approximately a 1° per degree change in the region of $\frac{bG_c c_{p,c}}{2U}$ of 5.

In tail-pipe burners cooled by air entering a cooling passage at 500°R and having combustion-gas temperatures of 1700° and 3500°R at the inlet and outlet, respectively, $\frac{bG_c c_{p,c}}{2U}$ has a value of approximately 5, and the possible variation in cooling-air temperature rise from the mean value of cooling-air temperature

rise is approximately ± 0.15 . For this region, a 4° change in outlet cooling-air temperature results in a 1° change in the maximum inside-wall temperature.

Rewritten in a working form, equation (19) is

$$\frac{bG_c c_{p,c}}{lU} = 50,000 \left(\frac{G_c}{G_g} \right)^{0.84} G_g^{0.29} \frac{b^{1.2}}{l} \left(\frac{1}{T_{g,2}} \right)^{0.38} \left(\frac{1}{T_{c,1}} \right)^{0.23} \quad (20)$$

Figure 5 in combination with the desired empirical equation (20) relates the outlet cooling-gas temperature to the independent variables.

Effect of Longitudinal Fins in Cooling Passage

The applicability of equation (19) has been investigated for a few combinations having fins attached to the burner wall. The exponents a and m in equation (19) were determined and found to be in agreement with the exponents in equation (20). The factor K in equation (19) was then determined using the remaining exponents of equation (20).

The form of equation (19), as indicated by figure 8, is applicable to longitudinal fins in the cooling passage when K is replaced by a function of the ratio of heat-transfer surface on the cooling-gas side including fins S_c to the heat-transfer surface on the combustion-gas side S_g of the inside wall. Figure 8 yields the approximate expression

$$K = 6100 \left(9.2 - \frac{S_c}{S_g} \right) \quad (21)$$

when the cooling passage contains fins of $1/16$ inch (0.0052 ft) thick Inconel having heights of $1/4$ to $1/2$ inch (0.02083 to 0.04167 ft) and spaced $1/2$ inch apart. A more thorough analysis is recommended for other combinations of materials and fin geometry.

Correction for External Heat Losses

Flight or test installations of tail-pipe burners that are not insulated may have appreciable heat loss through the outside

wall. In these cases, an approximate correction can be applied to the outlet cooling-gas temperature (obtained from equations (20) and (18)) before substitution into the parameter ψ . The heat loss from the outside wall to surroundings is

$$\frac{q}{S_o} = \sigma F_{A,E} (t_{o,av}^4 - T_0^4) + h_o (t_{o,av} - T_0) \quad (22)$$

where $t_{o,av}$ is the average outside-wall temperature and h_o is the outside-wall heat-transfer coefficient, which may be for free convection or forced convection depending on the installation. The heat-transfer coefficient for free convection about a horizontal cylinder is given in reference 8 as

$$h_o = 0.27 \left(\frac{t_{o,av} - T_0}{D_o} \right)^{0.25} \quad (23)$$

If the engine and tail-pipe burner are in an unconfined air stream of high velocity, h_o can be estimated from the flat-plate equation (reference 10) for turbulent flow,

$$h_o = 0.64 T_m^{0.3} \frac{(V_o \rho)^{0.8}}{l^{0.2}} \quad (24)$$

where l is the length of the plate. The reduction in outlet temperature of the cooling gas due to heat losses to the surroundings is

$$\Delta T_c = \left(\frac{q}{S_o} \right) \frac{S_o}{3600 W_c c_{p,c}} \quad (25)$$

and the corrected outlet cooling-gas temperature equals the outlet cooling-gas temperature without losses minus ΔT_c .

COMPARISON OF ANALYSIS WITH EXPERIMENT

Temperatures of the cooling-passage walls and the cooling gas have been measured on several tail-pipe burners during an investigation of their performance and operational characteristics in the NACA Lewis altitude wind tunnel. The method by which these data were obtained did not permit a direct check of the values of the factor K and the exponents in the empirical equation. A

preliminary check has been made, however, by comparing the experimentally observed temperatures with the corresponding temperatures calculated using the empirical equation. Typical results are presented for one of the tail-pipe burners, which is shown in figure 9, cooled by part of the turbine-outlet gas flowing through the annular cooling passage and by heat losses through the uninsulated outside wall (figs. 10 and 11). The heat losses to the tunnel test section were great enough that the outlet cooling-gas temperature was approximately equal to the inlet temperature. The outlet temperature of the cooling gas obtained from the empirical equation is therefore corrected for heat losses to the tunnel by the previously described method. In the calculations, the tunnel is considered to be a black body, the emissivity of the inside and outside walls is 0.7, nonluminous radiation is assumed from the combustion gas to the inside wall, and the characteristic length in equation (24) is 20 feet. (A sample calculation is given in appendix A.) The corrected cooling-gas temperature is used in determining the inside-wall temperature.

Comparison is made of the calculated and measured inside-wall and cooling-gas temperatures at the outlet of the 48-inch-long cylindrical section of the combustion chamber because temperatures were not measured in the nozzle section of the cooling passage. Inasmuch as the combustion-gas temperature at the outlet of the 48-inch section was not measured and because combustion continues in the nozzle, the combustion-gas temperature was estimated to equal the inlet combustion-gas temperature plus 0.85 of the combustion-temperature rise to the nozzle outlet.

Results and discussion. - Calculated and measured temperatures of the cooling gas and the inside wall are shown in figures 10 and 11. The corrected cooling-gas temperature is within $\pm 15^\circ$ of the measured cooling-gas temperature, and the calculated inside-wall temperature is within approximately $\pm 25^\circ$ of the measured inside-wall temperature. The difference between the measured and calculated inside-wall temperatures ranges from approximately 0.06 to 0.16 of the difference between the measured temperatures of the inside wall and the cooling gas.

The good agreement shown is due in part to the choice of combustion-gas temperature at the 48-inch station and the emissivity of the walls and of the ratio of luminous radiation to nonluminous radiation from the combustion gas to the inside wall. The effect of changes in the chosen values upon the agreement between calculated and measured temperatures will be subsequently

discussed. The agreement between the calculated and measured temperatures applies only to combustion chambers having a combination of a well-proportioned flame holder and an optimum fuel-injection system, which completely fills the burner cross section with flame and produces high combustion efficiencies. The analysis predicts cooling-gas and inside-wall temperatures that are too high for configurations in which fuel is concentrated near the center of the combustion chamber, or which have no flame holder, or when the radial clearance between the annular flame holder and the inside wall is large enough to provide a relatively cool layer of gas next to the inside wall.

Effects of uncertainties in calculated temperatures. - The accuracy to which the temperatures of the cooling gas and the inside wall can be calculated depends on the accuracy to which the quantities in the empirical equation and the parameters ϕ and ψ are known and in turn upon knowledge of actual conditions existing in the combustion chamber and the cooling passage.

The effects of several combinations of assumptions regarding combustion-gas temperature, emissivity, and ratio of luminous to nonluminous radiation on the computed temperatures at the outlet of the 48-inch section of the tail-pipe burner are shown in the following table. The measured quantities were: mass velocity of combustion gas, 6.83 pounds per second per square foot; mass velocity of cooling gas, 9.14 pounds per second per square foot; mass ratio W_c/W_g , 0.088; combustion-gas temperature at inlet, 1704° R; combustion-gas temperature at nozzle outlet, 3363° R; cooling-gas temperature at outlet of 48-inch section, 1712° R; average outside-wall temperature $t_{o,av}$, 1513° R; and inside-wall temperature $t_{i,2}$, 2130° R. The outside-wall heat-transfer coefficient h_o (equation (24)) is estimated from turbulent flow over a flat plate 20 feet long.

| | Meas- ured condi- tion | Assumed or calculated condition | | | | | | | |
|--|---------------------------------|---------------------------------|------|------|------|-------------------|------|------|------|
| | | | | | | | | | |
| Combustion-gas temperature, $T_{g,2}$, at 48-inch station, $^{\circ}\text{R}$ | | 3363 ^a | | | | 3114 ^b | | | |
| Theoretical outlet cooling-gas temperature, $^{\circ}\text{R}$ (equations (20) and (18)) | | 1853 | | | | 1830 | | | |
| Emissivity of cooling-passage wall, ϵ_w | | 0.7 | | 0.8 | | 0.7 | | 0.8 | |
| Corrected cooling-gas temperature, $T_{c,2}$, $^{\circ}\text{R}$ (equations (25), (22), and (24)) | 1712 | 1734 | | 1724 | | 1711 | | 1701 | |
| Radiation from gas to wall | | (c) | (d) | (c) | (d) | (c) | (d) | (c) | (d) |
| Inside-wall temperature, $t_{1,2}$, $^{\circ}\text{R}$ (equation (13)) | 2130 | 2215 | 2315 | 2188 | 2290 | 2118 | 2195 | 2094 | 2185 |

^aCombustion-gas temperature at nozzle outlet.

^bInlet combustion-gas temperature plus 0.85 combustion-temperature rise to nozzle outlet.

^cNonluminous radiation from combustion gas to inside wall.

^dTwo times nonluminous radiation from combustion gas to inside wall.

The preceding table shows that either of the assumed temperatures for combustion gas at the outlet of the 48-inch section gave corrected cooling-gas temperatures close to the measured temperature of 1712 $^{\circ}$ R. The temperatures of the cooling gas and of the inside wall are approximately 23 $^{\circ}$ and 100 $^{\circ}$ higher, respectively, when the temperature at the nozzle outlet is assumed at the 48-inch station.

An increase in ϵ_w from 0.7 to 0.8 lowers the outlet cooling-gas temperature 10 $^{\circ}$ R and lowers the inside-wall temperature 10 $^{\circ}$ to

27° R. It is therefore concluded that the choice of wall emissivity is of secondary consideration in the region of ϵ_w equal to about 0.7 or 0.8. Doubling the nonluminous radiation from the combustion gas increases the inside-wall temperature from about 80° to 100° R.

Obviously, a number of combinations of assumptions, within certain limits, will yield calculated temperatures equally close to the measured temperatures. The proper choice, however, depends on more precise knowledge of the actual conditions. Uncertainties in the actual combustion-gas temperature near the inside wall are most critical and should be experimentally investigated for various combinations of flame holder and fuel-injection system. The ratio of luminous radiation to nonluminous radiation from the combustion gases is of equal importance, although more difficult to determine experimentally.

SUMMARY OF RESULTS

An analysis has been made that reduces the labor of calculating the maximum inside-wall temperature of the combustion chamber of a tail-pipe burner or a ram-jet combustion chamber cooled by air or gas flowing through a surrounding annular cooling passage. The maximum temperature of the inside wall is obtained from a heat balance across the inside wall at the outlet after the outlet temperature of the cooling gas has been determined from other known conditions. The calculation of the inside-wall temperature from the heat balance requires the solution of a fourth-degree algebraic equation, which is simplified by means of a working chart.

Because the outlet temperature of the cooling gas $T_{c,2}$ is not generally known, an empirical equation is developed that relates the outlet cooling-gas temperature to known temperatures, flow conditions, and geometry. The empirical equation is

$$\frac{bG_c c_{p,c}}{2U} = K \left(\frac{G_c}{G_g} \right)^{0.84} G_g^{0.29} \frac{b^{1.2}}{l} T_{g,2}^{-0.38} T_{c,1}^{-0.23} \quad (20)$$

where

b cooling-passage height, (ft)

$c_{p,c}$ specific heat at constant pressure of cooling gas,
(Btu/(lb)(°R))

- G_c mass velocity of cooling gas, (lb/(sec)(sq ft))
 G_g mass velocity of combustion gas, (lb/(sec)(sq ft))
 l length, (ft)
 $T_{c,1}$ inlet cooling-gas temperature, ($^{\circ}$ R)
 $T_{g,2}$ outlet cooling-gas temperature, ($^{\circ}$ R)
 U effective over-all heat-transfer coefficient

The factor K in equation (20) is shown to be a function of the ratio of heat-transfer surface on the cooling-gas side S_c to the heat-transfer surface on the combustion-gas side S_g . For longitudinal fins of 1/16 inch thick Inconel spaced 1/2 inch apart and having heights of 1/4 to 1/2 inch,

$$K = 6100 \left(9.2 - \frac{S_c}{S_g} \right) \quad (21)$$

which reduces to 50,000 for an unfinned annular passage where S_c/S_g equals unity.

A combination of equation (20) with the characteristic equation (18)

$$\frac{T_{g,2} - T_{c,2}}{T_{g,2} - T_{g,1}} = \frac{1 - \left[1 - \frac{T_{g,1} - T_{c,1}}{T_{g,2} - T_{g,1}} \left(\frac{lU}{bG_c c_{p,c}} \right) \right] e^{-\frac{lU}{bG_c c_{p,c}}}}{\frac{lU}{bG_c c_{p,c}}} \quad (18)$$

gives the unknown outlet cooling-gas temperature in terms of known temperatures, mass flows, and geometry.

Temperatures calculated by this analysis and the selected assumptions show good agreement with corresponding temperatures measured on several experimental tail-pipe burners. Calculated cooling-gas temperatures at a station 0.7 of the distance from the flame holder to the nozzle outlet are within $\pm 15^{\circ}$ of the corresponding measured temperatures; and calculated inside-wall temperatures are within approximately $\pm 25^{\circ}$ of the corresponding measured temperatures. The difference between the measured and calculated temperatures of the inside wall ranges from about 0.06 to 0.16 of the difference between the measured temperatures of the inside wall and the cooling gas.

The agreement shown applies only to combustion chambers having a combination of well-proportioned flame holders and an optimum fuel-injection system, which results in a complete filling of the burner cross section with flame and a high combustion efficiency.

The analysis predicts temperatures that are too high for configurations in which the fuel is concentrated near the center of the combustion chamber, or that have no flame holder, or where the radial clearance between the flame holder and the inside wall is large enough to provide a relatively cool layer of gas between the flames and the wall.

Lewis Flight Propulsion Laboratory,
National Advisory Committee for Aeronautics,
Cleveland, Ohio.

APPENDIX A

SAMPLE CALCULATION

The inside-wall temperature is calculated for a typical set of conditions obtained on an experimental tail-pipe burner. Radiation from the combustion gas is assumed to be twice the nonluminous radiation and the outside-wall heat-transfer coefficient is estimated from turbulent flow over a flat plate 20 feet long.

Given conditions. - The following quantities are assumed to be known:

| | |
|--|-------|
| Burner length, l , in. | 48 |
| Outside diameter of inside wall, D_i , in. | 31 |
| Inside diameter of outside wall, D_o , in. | 32 |
| Mass flow of cooling gas, W_c , lb/sec | 3.14 |
| Mass flow of combustion gas, W_g , lb/sec | 35.78 |
| Tunnel airspeed, V_o , ft/sec | 140 |
| Tunnel air temperature, T_o , $^{\circ}\text{R}$ | 504 |
| Tunnel static pressure, p_o , lb/sq ft absolute | 781 |
| Combustion-gas temperature T_g at nozzle outlet, $^{\circ}\text{R}$. . . | 3363 |
| Static pressure of combustion gas at 48-inch station, lb/sq ft absolute | 1240 |

The following temperatures were measured on the 48-inch section of the combustion chamber:

| Measured tempera- ture | Temperature ($^{\circ}\text{R}$) | |
|------------------------------|---------------------------------------|-------------------|
| | Inlet station | Outlet station |
| t_o | 1488 | 1538 |
| T_c | 1711 | 1712 |
| t_i | 1744 | 2130 |
| T_g | 1704 | ^a 3114 |

^aTaken as inlet combustion-gas temperature plus 0.85 of combustion-gas temperature rise to nozzle outlet.

Hydraulic diameters and passage height. - The hydraulic diameter of the annular cooling passage is obtained from equation (4)

$$D_c = \frac{1}{12} = 0.08333 \text{ ft}$$

and the hydraulic diameter of the combustion-gas passage equals the geometrical diameter D_i

$$D_g = D_i = \frac{31}{12} = 2.583 \text{ ft}$$

The cooling-passage height is

$$b = \frac{1}{2} D_c = 0.04167 \text{ ft}$$

Flow areas and mass velocities. - The flow areas of the cooling passage and the combustion chamber are, respectively,

$$A_c = \frac{\pi}{4} \frac{(32^2 - 31^2)}{144} = 0.3435 \text{ sq ft}$$

$$A_g = \frac{\pi}{4} 2.583^2 = 5.24 \text{ sq ft}$$

from which the respective mass velocities are

$$G_c = \frac{3.14}{0.3435} = 9.14 \text{ lb/((sec)(sq ft))}$$

$$G_g = \frac{35.78}{5.24} = 6.83 \text{ lb/((sec)(sq ft))}$$

Radiation between walls. - The inside and outside walls of the cooling passage were Inconel, which had an emissivity ϵ_w of about 0.7 for the surface conditions and temperatures encountered (reference 8). The corresponding value of ϵ'_w is 0.85 (equation (6)).

From equation (8),

$$F_{A,E} = \frac{1}{\frac{1}{0.7} + \left(\frac{31}{32}\right)\left(\frac{1}{0.7} - 1\right)} = 0.543$$

Radiation from combustion gas. - The nonluminous radiation from the combustion gas is calculated from data in reference 8 by

assuming complete combustion of a stoichiometric mixture of $C_{12}H_{26}$, for which the ratio of partial pressures of the carbon dioxide and water vapor to the static pressure of the combustion products are, respectively,

$$\frac{p_{CO_2}}{p_g} = 0.1388$$

and

$$\frac{p_{H_2O}}{p_g} = 0.1276$$

The beam length L is taken as 0.8 of the combustion-chamber diameter (reference 8, p. 69). The product

$$p_g L = \frac{0.8 \times 1240 \times 2.583}{2116} = 1.21 \text{ foot atmosphere}$$

and

$$p_{CO_2} L = 1.21 \times 0.1388 = 0.168$$

$$p_{H_2O} L = 1.21 \times 0.1276 = 0.154$$

$$p_{CO_2} L + p_{H_2O} L = 0.322$$

The partial pressures of the carbon dioxide and water vapor in atmospheres are

$$p_{CO_2} = \frac{1240}{2116} \times 0.1388 = 0.081$$

$$p_{H_2O} = \frac{1240}{2116} \times 0.1276 = 0.075$$

and

$$\frac{p_{H_2O}}{p_{H_2O} + p_{CO_2}} = 0.48$$

As an initial estimate, let $t_{1,2} = 2150^\circ \text{ R} = 1690^\circ \text{ F}$ and from the given conditions, $T_{g,2} = 3114^\circ \text{ R} = 2654^\circ \text{ F}$ for which

$$\epsilon_{\text{CO}_2} = 0.057 \quad \alpha_{\text{CO}_2} = 0.089$$

$$\epsilon_{\text{H}_2\text{O}} = 0.039 \quad \alpha_{\text{H}_2\text{O}} = 0.067$$

$$C_1 = 1.05$$

$$C_1 \epsilon_{\text{H}_2\text{O}} = 0.041 \quad C_1 \alpha_{\text{H}_2\text{O}} = 0.070$$

$$\Delta \epsilon = 0.005 \quad \Delta \alpha = 0.004$$

$$\epsilon_g = 0.093 \quad \alpha_g = 0.155$$

Use of empirical equation. - From equation (20),

$$\begin{aligned} \frac{bG_c c_{p,c}}{lU} &= 50,000 \left(\frac{G_c}{G_g} \right)^{0.84} G_g^{0.29} \frac{b^{1.2}}{l} T_{g,2}^{-0.38} T_{c,1}^{-0.23} \quad (20) \\ &= 50,000 \left(\frac{9.14}{6.83} \right)^{0.84} \times 6.83^{0.29} \times \frac{0.04167^{1.2}}{4} \times 3114^{-0.38} \times 1711^{-0.23} \\ &= 5.21 \end{aligned}$$

and from the zero curve of $\frac{T_{g,1} - T_{c,1}}{T_{g,2} - T_{g,1}}$ in figure 5,

$$\frac{T_{g,2} - T_{c,2}}{T_{g,2} - T_{g,1}} = 0.91$$

Therefore,

$$T_{c,2} = 3114 - 0.91(3114 - 1704) = 1830^\circ \text{ R}$$

Correction of cooling-gas temperature for heat losses. - The outside-wall heat-transfer coefficient is estimated from equation (24):

$$h_o = 0.64 T_m^{0.3} \frac{(V_{op})^{0.8}}{l^{0.2}} \quad (24)$$

where

$$T_m = \frac{t_{o,av} + T_0}{2}$$

$$= \frac{1}{2} \left(\frac{1488 + 1538}{2} + 504 \right) = 1008^\circ \text{ R}$$

and

$$\rho = \frac{781}{53.3 \times 1008} = 0.0145 \text{ lb/cu ft}$$

The value of l , taken as the length of engine plus tail-pipe burner, is 20 feet.

$$h_o = 0.64 \times 1008^{0.3} \times \frac{(140 \times 0.0145)^{0.8}}{20^{0.2}} = 4.95 \text{ Btu/(hr)(sq ft)(}^\circ\text{R)}$$

From equation (22)

$$\frac{q}{S_o} = 0.173 \times 10^{-8} \times 0.7 \left[\left(\frac{1488 + 1538}{2} \right)^4 - 504^4 \right] +$$

$$4.95 \left(\frac{1488 + 1538}{2} - 504 \right)$$

$$= 11,260 \text{ Btu/(hr)(sq ft)}$$

and from equation (25)

$$\Delta T_c = \frac{11,260 \times \pi \times \frac{32}{12} \times 4}{3600 \times 3.14 \times 0.28} = 119^\circ \text{ R}$$

The corrected cooling-gas temperature is

$$T_{c,2} = 1830 - 119 = 1711^\circ \text{ R}$$

Heat-transfer coefficient. - Equation (2) gives the heat-transfer coefficient for the cooling gas as

$$h_o = 0.378 \times \frac{1711^{0.3} \times 9.14^{0.8}}{0.0833^{0.2}} = 34.1 \text{ Btu/(hr)(sq ft)(}^\circ\text{R)}$$

and for the combustion gas as

$$h_g = 0.378 \times \frac{3114^{0.3} \times 6.83^{0.8}}{2.583^{0.2}} = 16.27 \text{ Btu/(hr)(sq ft)(}^{\circ}\text{R)}$$

Determination of inside-wall temperature. - From equations (16) and (17),

$$\psi = \frac{3114^4 \times 0.173 \times 10^{-8} \times 0.85 \times 2 \times 0.093 + 3114 \times 16.27 + 1711^4 \times 0.173 \times 10^{-8} \times 0.543 + 1711 \times 34.1}{16.27 + 34.1}$$

= 2836

$$\phi = \frac{0.173 \times 10^{-8} (0.543 + 0.85 \times 2 \times 0.155) 2836^3}{16.27 + 34.1} = 0.637$$

for which figure 4 gives $t_1/\psi = 0.774$

The calculated inside-wall temperature is

$$t_{1,2} = 2836 \times 0.774 = 2195^{\circ} \text{ R}$$

which is close enough to the initial estimate of wall temperature that a reestimation is unnecessary.

APPENDIX B

DERIVATION OF LONGITUDINAL DISTRIBUTION OF
COOLING-GAS TEMPERATURE

The one-dimensional distribution of cooling-gas temperature will be derived for the case of constant over-all heat-transfer coefficient U , a linear combustion-gas temperature distribution, and no heat lost to the outside. With reference to figure 1, the general case when $T_{g,1}$ and $T_{c,1}$ are different is considered. It is then assumed that at some station upstream (where $x = 0$) $T_g = T_c = T_o$. The linear distribution in combustion-gas temperature is expressed by

$$\frac{dT_g}{dx} = \beta \quad (B1)$$

The heat balance across a small segment dx of the inside wall gives

$$W_c c_{p,c} dT_c = U(T_g - T_c) \pi D_i dx \quad (B2)$$

Using the simplifying notation that

$$B = \frac{W_c c_{p,c}}{U \pi D_i} = \frac{b G_c c_{p,c}}{U} \quad (B3)$$

equations (B1), (B2), and (B3) combine to give

$$\frac{d(T_g - T_c)}{dx} + \frac{(T_g - T_c)}{B} = \beta \quad (B4)$$

which has the solutions

$$(T_{g,1} - T_{c,1}) = B\beta \left(1 - e^{-\frac{x_1}{B}} \right) \quad (B5)$$

and

$$(T_{g,2} - T_{c,2}) = B\beta \left(1 - e^{-\frac{x_2}{B}} \right) \quad (B6)$$

By rearrangement and subtraction of equation (B5) from equation (B6)

$$\frac{1}{B} = \frac{x_2}{B} - \frac{x_1}{B} = \log_e \left(1 - \frac{T_{g,1} - T_{c,1}}{B\beta} \right) - \log_e \left(1 - \frac{T_{g,2} - T_{c,2}}{B\beta} \right) \quad (B7)$$

However,

$$\frac{1}{B\beta} = \frac{1}{B} \left(\frac{1}{\beta} \right) = \frac{1}{B} \frac{1}{(T_{g,2} - T_{g,1})} = \frac{1U}{bG_c c_{p,c}} \frac{1}{(T_{g,2} - T_{g,1})}$$

and equation (B7) can be rewritten as

$$\frac{T_{g,2} - T_{c,2}}{T_{g,2} - T_{g,1}} = \frac{1 - \left[1 - \frac{T_{g,1} - T_{c,1}}{T_{g,2} - T_{g,1}} \left(\frac{1U}{bG_c c_{p,c}} \right) \right] e^{-\frac{1U}{bG_c c_{p,c}}}}{\frac{1U}{bG_c c_{p,c}}} \quad (B8)$$

which relates the outlet temperature of the cooling gas to U and the known variables.

REFERENCES

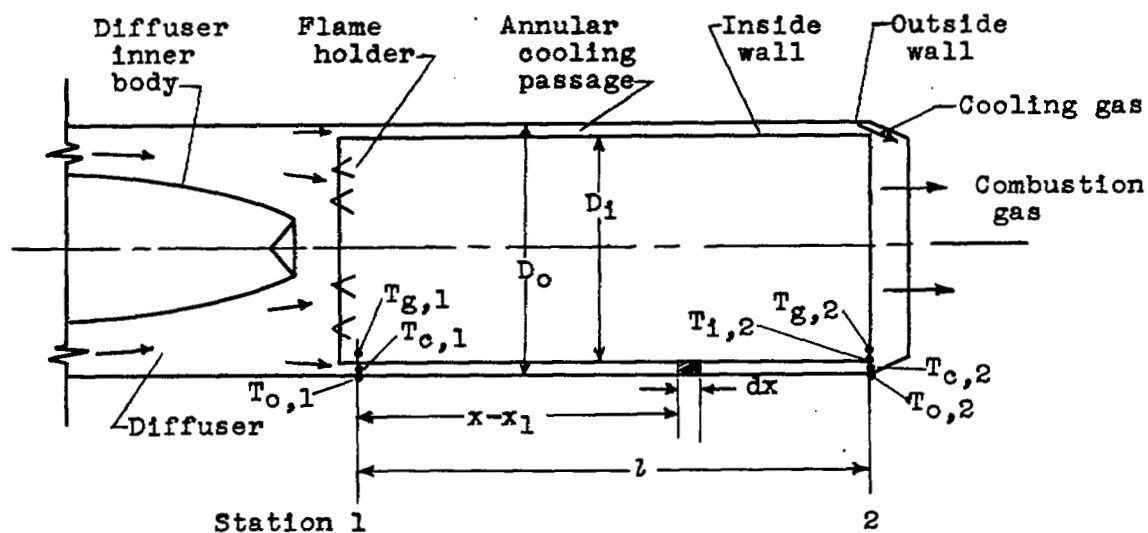
1. Anon.: Engineering Properties of Inconel. Bull. T-7, Development and Res. Div., The International Nickel Co., Inc., March 1943.
2. Shepherd, T. L.: An Investigation of the Structure Temperatures in the Combustion Chamber of the P/A VI. Rep. No. 5662, Eng. Dept., Chance Vought Aircraft, July 21, 1947.
3. Perchonok, Eugene, Sterbentz, William H., and Wilcox, Fred A.: Performance of a 20-Inch Steady-Flow Ram Jet at High Altitudes and Ram Pressure Ratios. NACA RM E6L06, 1947.
4. Perchonok, Eugene, Wilcox, Fred A., and Sterbentz, William H.: Investigation of the Performance of a 20-Inch Ram Jet Using Preheated Fuel. NACA RM E6I23, 1946.
5. Woodward, William H., and Bobrowsky, A. R.: Preliminary Investigation of a Ceramic Lining for a Combustion Chamber for Gas-Turbine Use. NACA RM E7H20, 1948.
6. Williams, D. T., and Dunlap, R. A.: Equilibrium Temperature of a Ram-Jet Burner Shell. External Memo. No. 12, Dept. Eng. Res., Univ. Mich., Nov. 10, 1947. (AAF Contract W33-038 ac-14222, Proj. MX-794, ATI 19218.)
7. Ellerbrock, Herman H., Jr., Wcislo, Chester R., and Dexter, Howard E.: Analysis, Verification, and Application of Equations and Procedures for Design of Exhaust-Pipe Shrouds. NACA TN 1495, 1947.
8. McAdams, William H.: Heat Transmission. McGraw-Hill Book Co., Inc., 2d ed, 1942.
9. Haslam, R. T., and Boyer, M. W.: Radiation from Luminous Flames. Ind. and Eng. Chem., vol. 19, no. 1, Jan. 1927, pp. 4-6.

10. Boelter, L. M. K., Martinelli, R. C., Romie, F. E., and Morrin, E. H.: An Investigation of Aircraft Heaters. XVIII - A Design Manual for Exhaust Gas and Air Heat Exchangers. NACA ARR 5A06, 1945.
11. Dobbins, John P.: Final Report on the Development of Thermal Insulation for Jet Engine Exhaust Systems. Rep. No. NA-47-1122, North American Aviation, Inc., Dec. 31, 1947. (Bur. Aero. Contract NOa(s)8474.)
12. Boelter, L. M. K., Cherry, V. H., Johnson, H. A., and Martinelli, R. C.: Heat Transfer Notes. Univ. Calif. Press (Berkeley), 1948, p. II b-12.

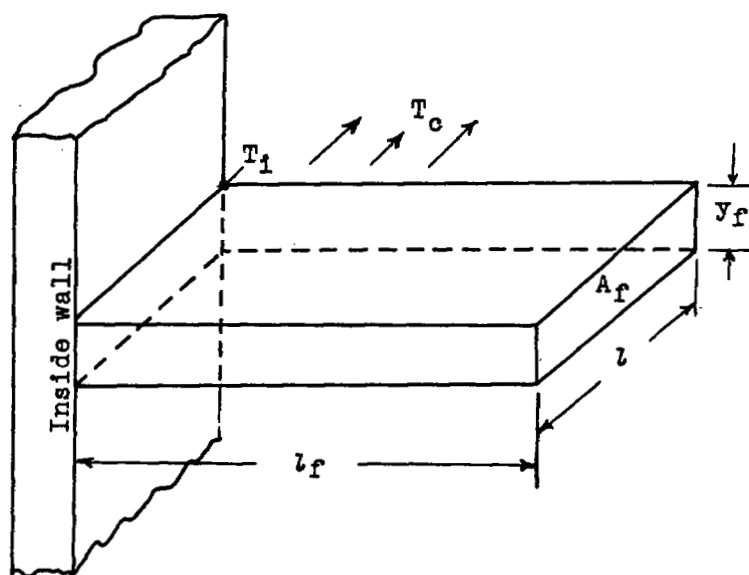
TABLE I - TABULATION OF CONFIGURATIONS AND VARIABLES INVESTIGATED WITH STEP-BY-STEP METHOD



| Symbol | Burner diameter D_1 (ft) | Passage height b (ft) | Burner length L (ft) | Mass velocity of combustion gas G_g (lb/(sec)(sq ft)) | Mass velocity ratio G_c/G_g | Mass ratio W_c/W_g | Diffuser total pressure P_d (lb/sq ft abs.) | Inlet total temperature | | Outlet total temperature | | Maximum inside-wall temperature t_1 (°R) | Fins |
|--------|----------------------------------|-------------------------------|------------------------------|---|---|---|---|-------------------------|-------------------|--|---|--|------|
| | | | | | | | | $T_{c,1}$ (°R) | $T_{g,1}$ (°R) | Combustion gas $T_{g,2}$ (°R) | Cooling gas $T_{c,2}$ (°R) | | |
| ○ | 0.8333 | 0.01042 | 5 | 10 | 0.394 .788 1.181 1.575 | 0.02 .04 .06 .08 | 1458 | 500 | 500 | 3500 | 2370 1799 1519 1345 | 2655 2298 2101 1954 | No |
| □ | 0.8333 | 0.04167 | 5 | 10 | 0.4 .8 1.18 1.57 | 0.0641 .1683 .2488 .330 | 1458 | 500 | 500 | 3500 | 1096 855 762 713 | 2190 1995 2170 1785 | No |
| ◇ | 1.667 | 0.01563 | 5 | 10 | 0.533 1.065 1.598 | 0.02 .04 .06 | 1458 | 500 | 500 | 3500 | 1719 1273 1083 | 2325 2038 1860 | No |
| △ | 1.667 | 0.02083 | 5 | 3.9 | 0.393 .785 1.18 1.57 | 0.02 .04 .06 .08 | 568 | 500 | 500 | 3500 | 2035 1478 1175 1068 | 2330 2060 1890 1765 | No |
| ▽ | 1.667 | 0.02083 | 5 | 6.35 | 0.502 1.0 1.4 | 0.03 .05 .07 | 979 | 443 | 443 | 3463 | 1475 1160 1004 | 2183 2000 1897 | No |
| ◁ | 1.667 | 0.08083 | 5 | 10 | 0.393 .393 .785 1.18 1.18 .3 .7 1.0 1.405 | 0.0196 .0196 .0392 .0588 .0588 .01496 .0549 .05 .0698 | 1458 | 500 | 500 | 2000 2500 2500 2500 3000 3500 | 987 1189 930 834 944 1896 1270 1115 980 | 1520 1819 1825 1500 1750 2451 2146 2000 1878 | No |
| ▷ | 1.667 | 0.02083 | 5 | 21.25 | 0.393 .785 1.18 1.57 | 0.02 .04 .06 .08 | 3850 | 638 | 638 | 3608 | 1593 1237 1093 997 | 2430 2200 2085 1990 | No |
| ▽ | 1.667 | 0.02083 | 5 | 32.2 | 0.783 .783 .393 .785 1.18 1.571 | 0.04 .04 .02 .04 .06 .08 | 4900 | 670 | 670 | 2000 2500 3630 | 898 980 1501 1218 1068 994 | 1410 1702 2520 2270 2060 1930 | No |
| ▷ | 1.667 | 0.04167 | 5 | 10 | 0.3 .5 .7 1.0 1.3 | 0.03065 .05108 .0716 .1021 .1328 | 1458 | 500 | 500 | 3500 | 1240 1003 906 796 732 | 2275 2169 2021 1975 1887 | No |



(a) Notation for combustion chamber and cooling passage.



(b) Notation for longitudinal fin: $A_f = y_f l$;
 $C = 2l$; $S_c = (s + 2l_f)l$.

Figure 1. - Schematic diagram of combustion chamber and longitudinal fin.

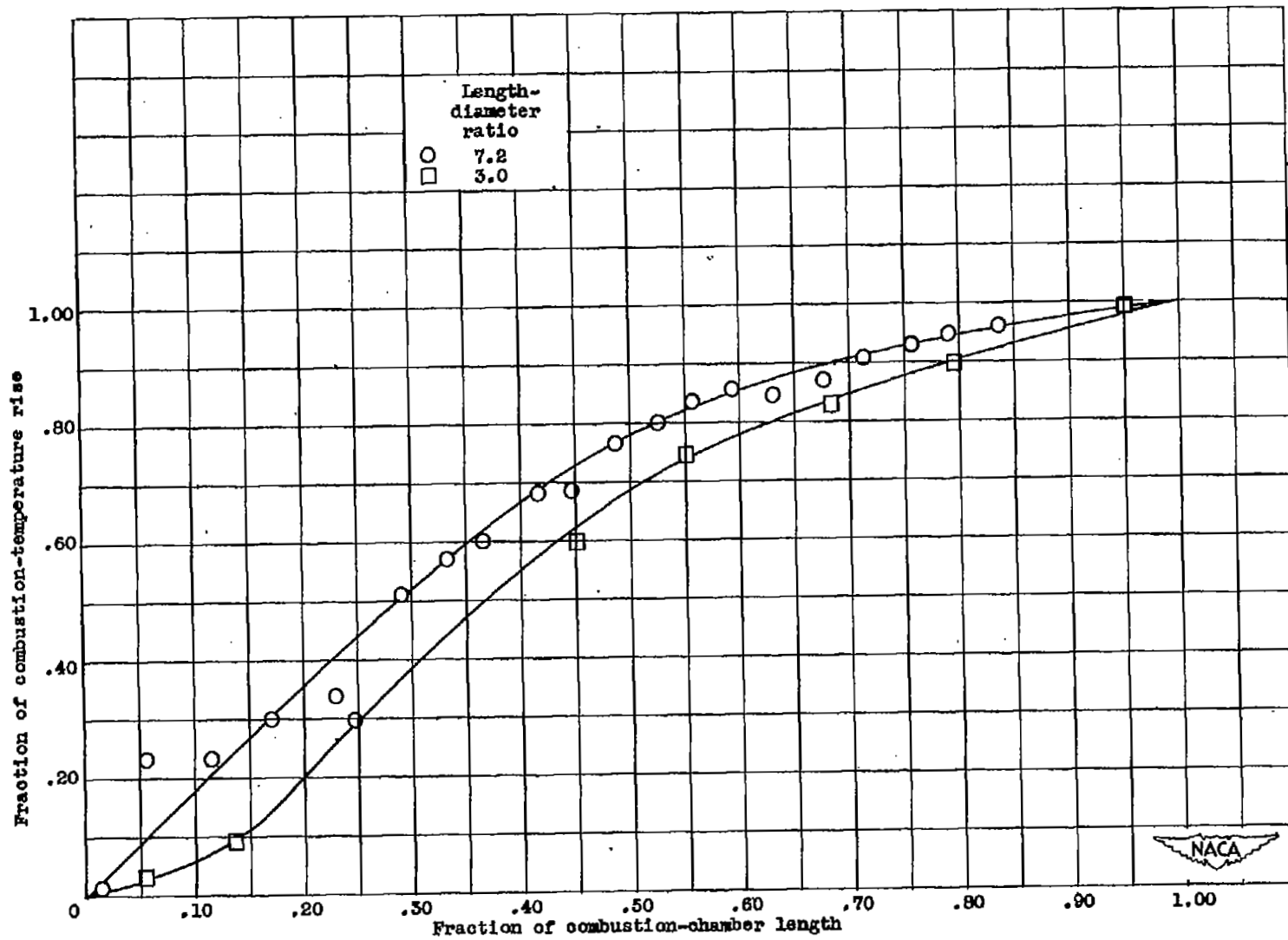


Figure 2. - Distribution of mean combustion-gas temperature determined from measured static-pressure distribution.

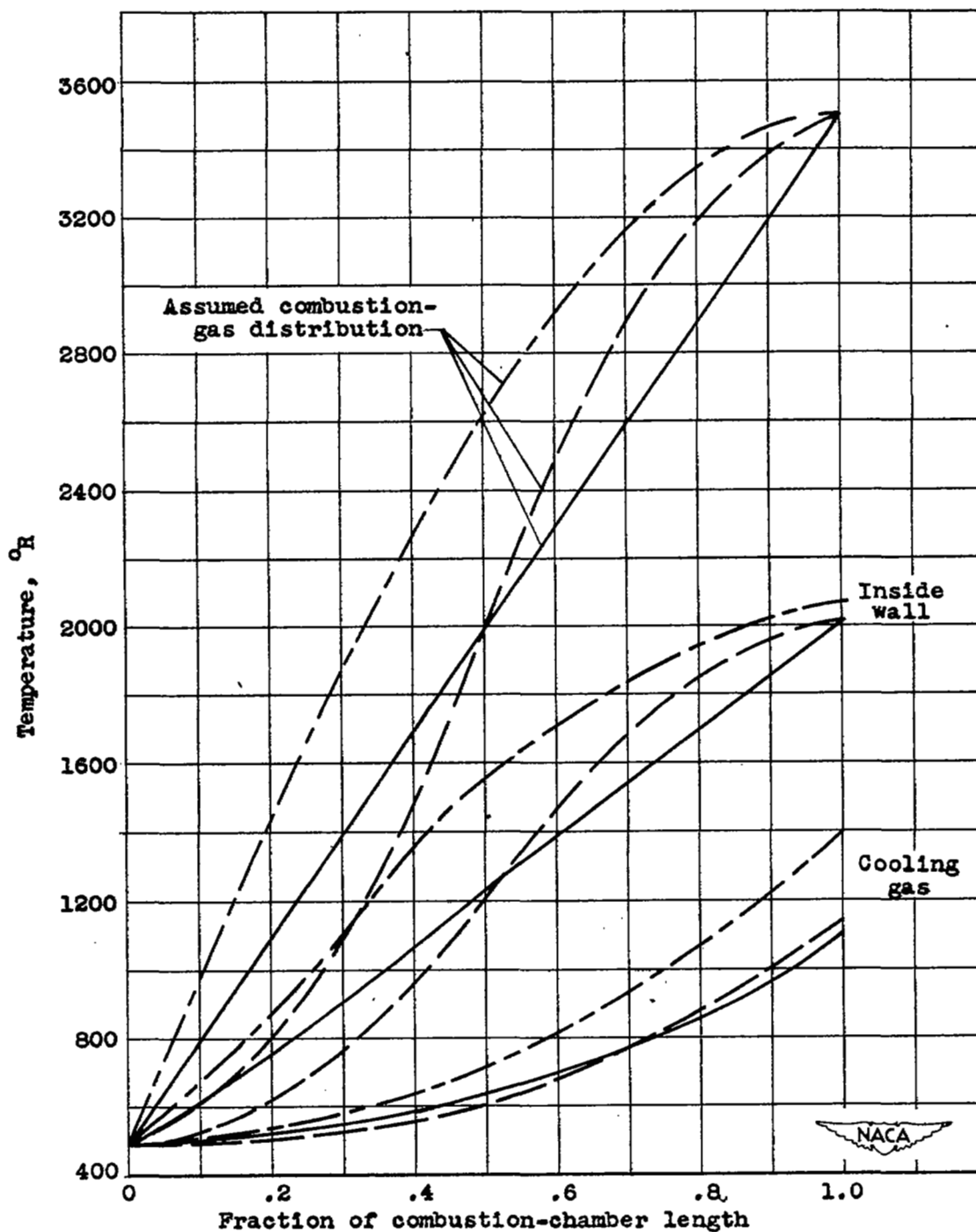


Figure 3. - Effect of assumed distribution of combustion-gas temperature on temperature of inside wall and cooling gas.

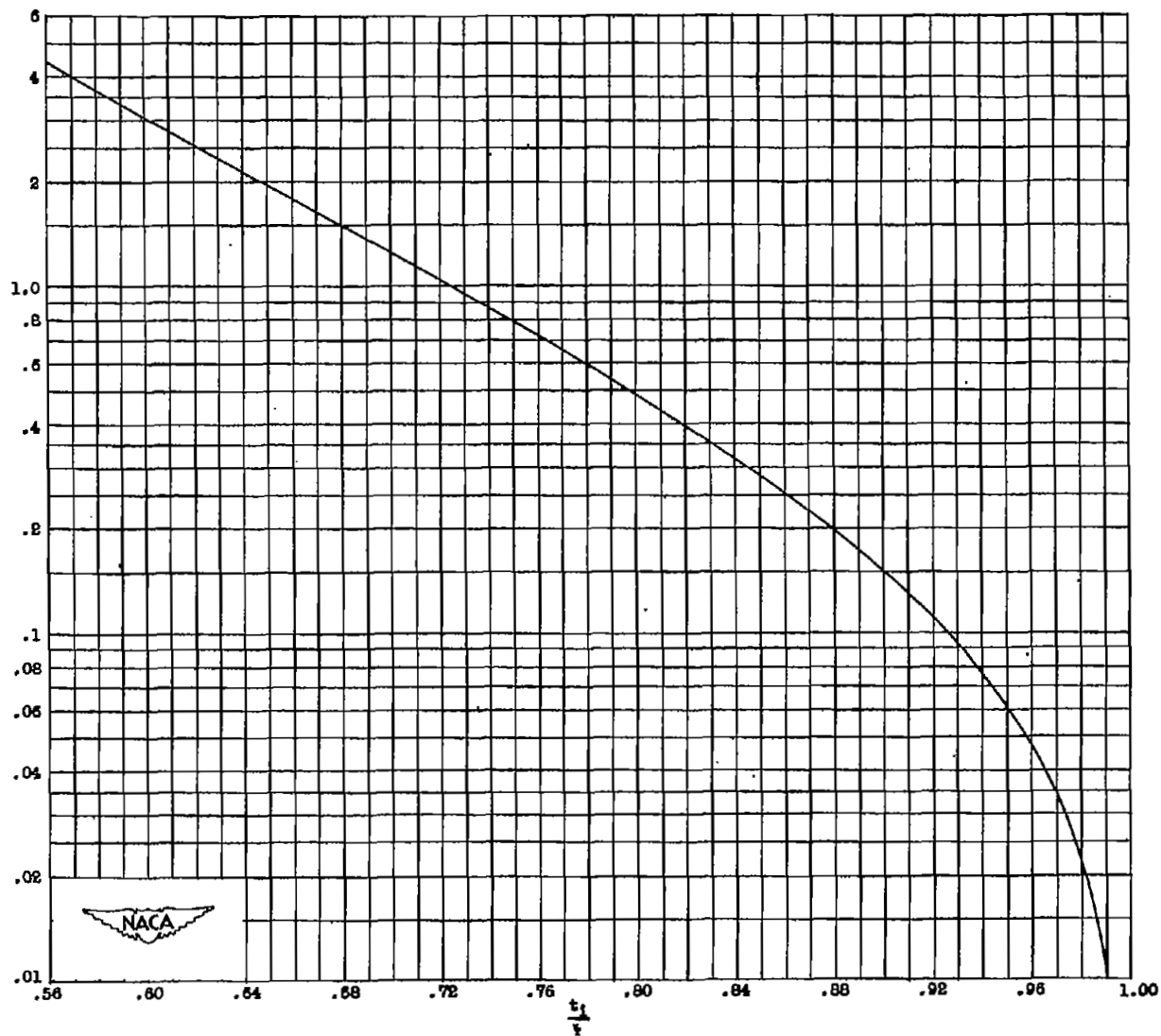


Figure 4. - Plot of equation (13), $\varphi\left(\frac{t_1}{y}\right)^4 + \left(\frac{t_1}{y}\right) = 1$.

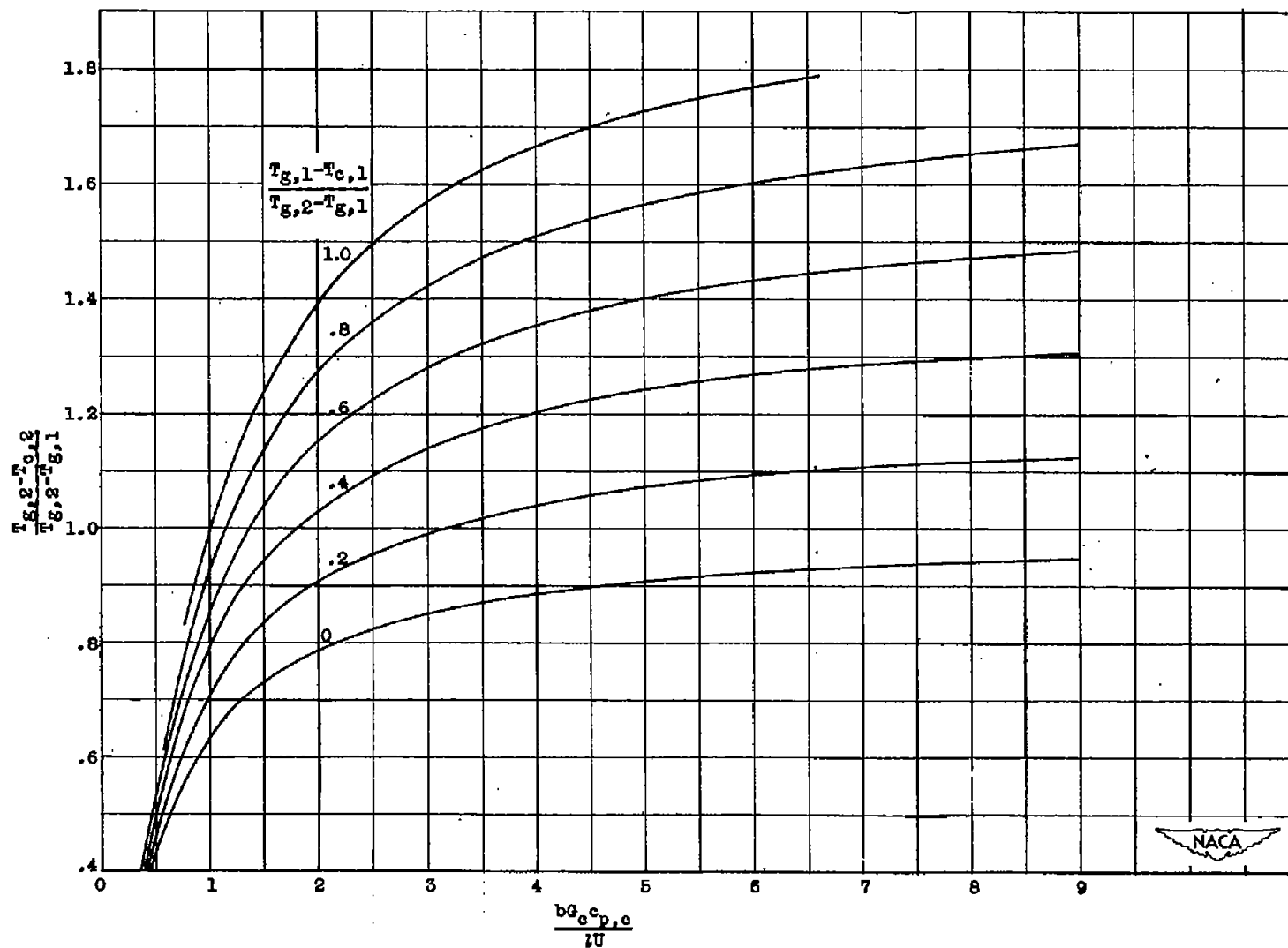


Figure 5. - Performance characteristics of parallel-flow heat exchanger having linear rise in combustion-gas temperature and constant effective over-all heat-transfer coefficient.

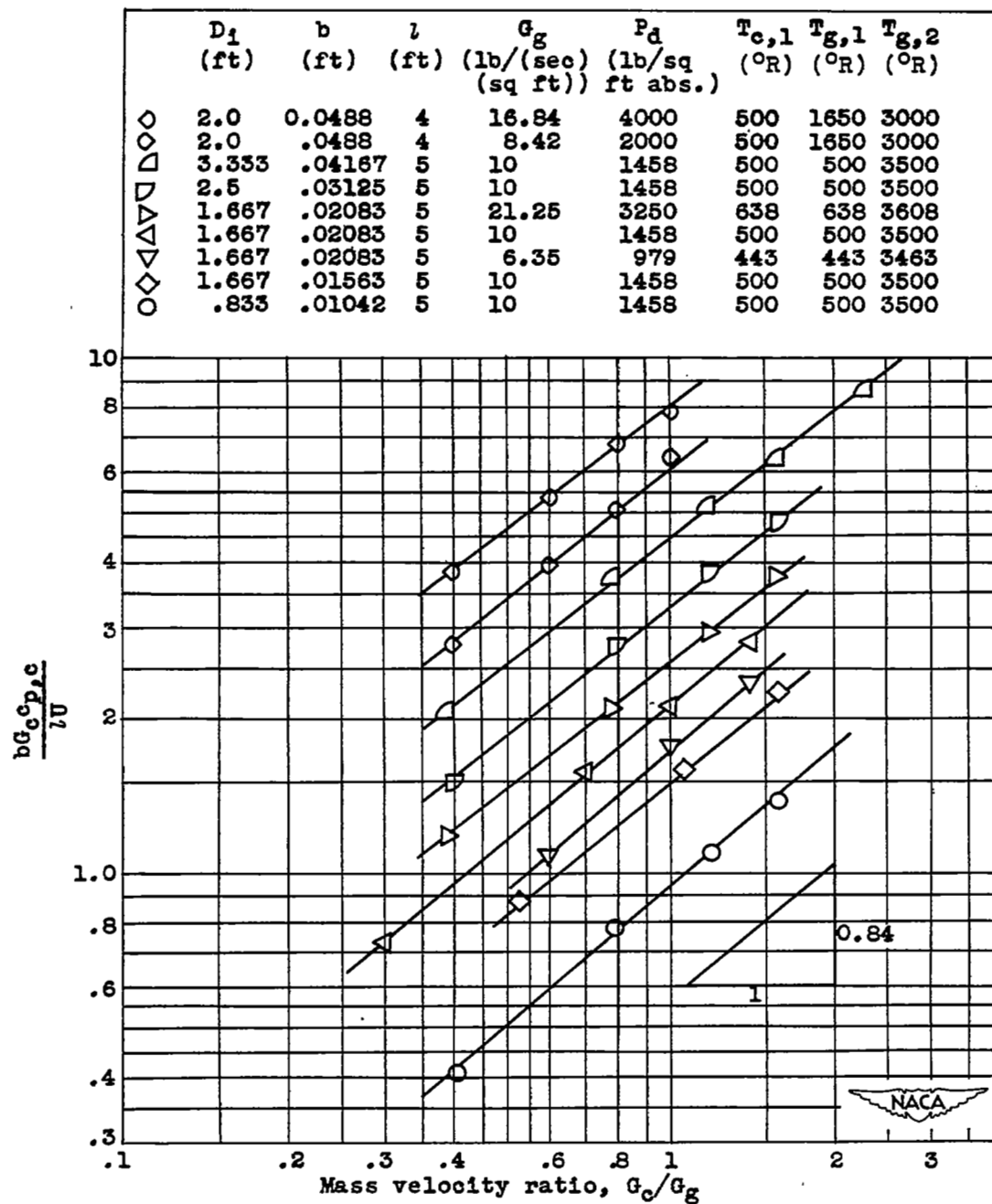


Figure 6. - Determination of exponents in empirical equation (19).

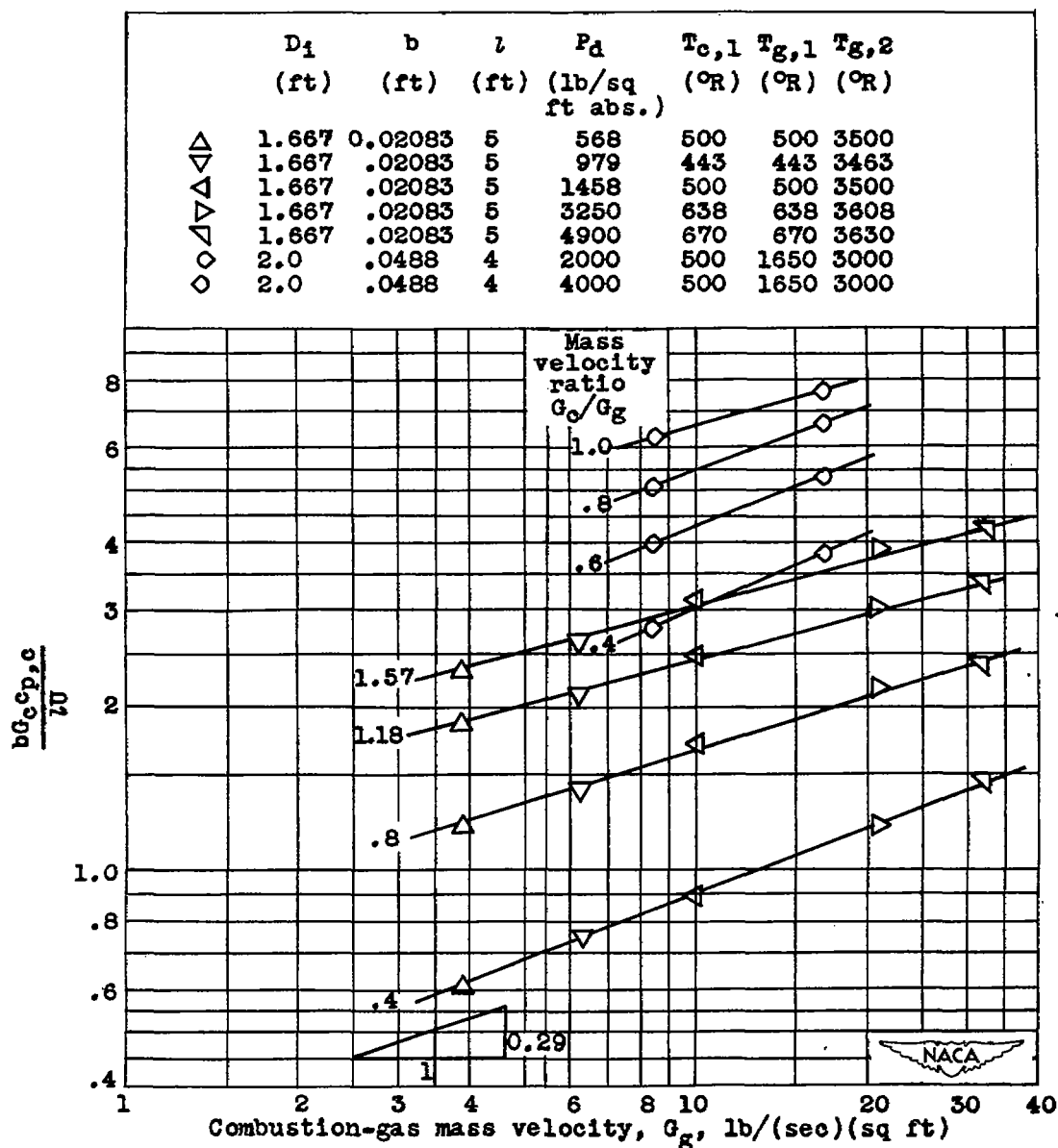
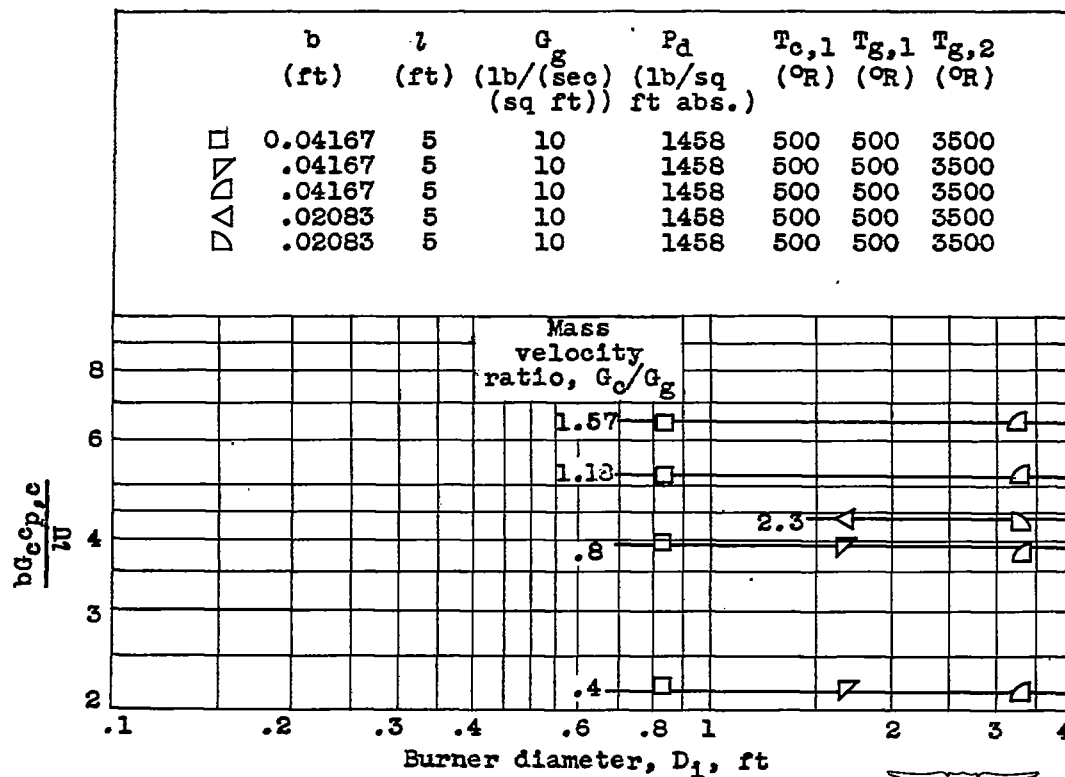


Figure 6. - Continued. Determination of exponents in empirical equation (19).



(c) Determination of j .

Figure 6. - Continued. Determination of exponents in empirical equation (19).

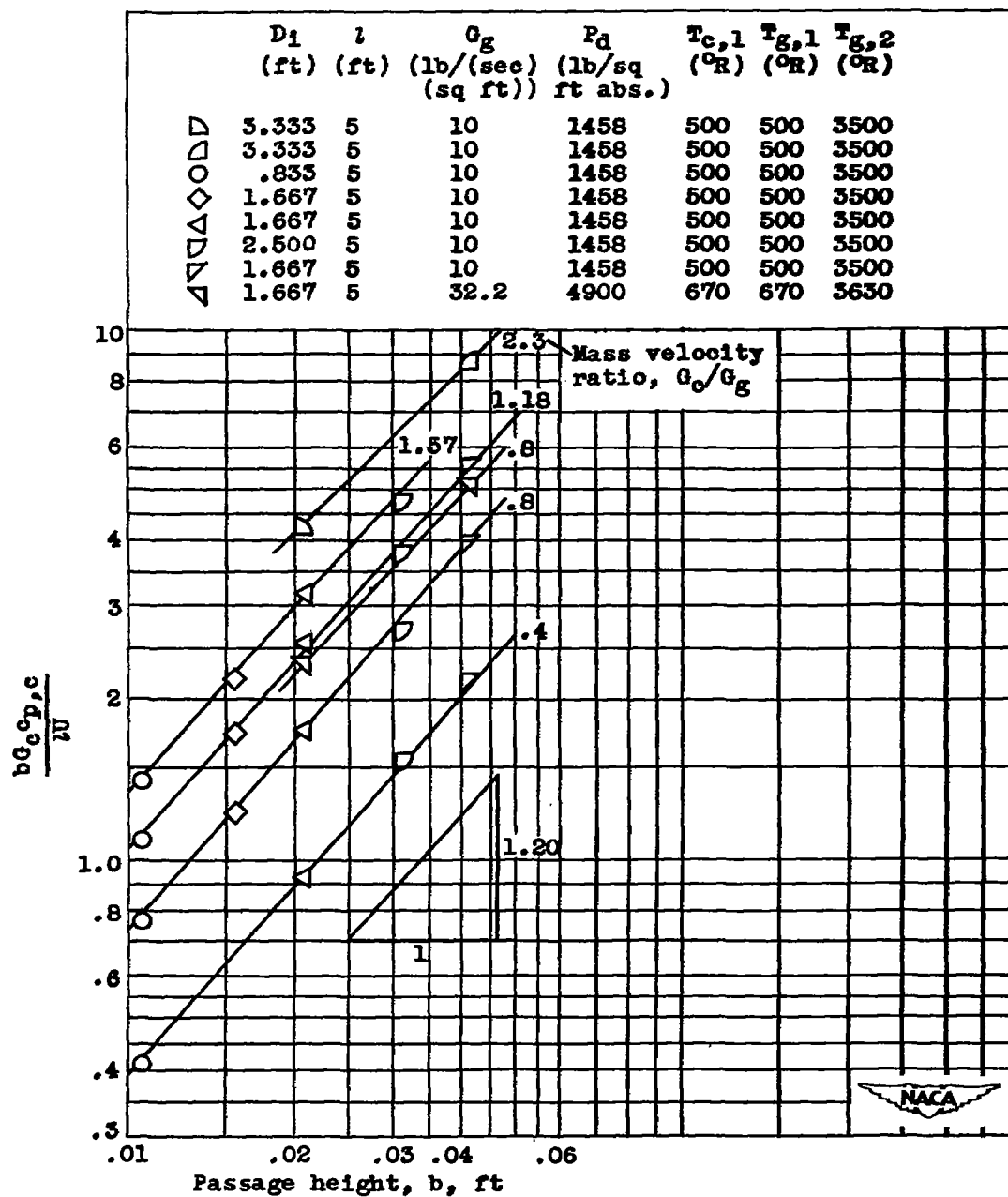
(d) Determination of m .

Figure 6. - Continued. Determination of exponents in empirical equation (19).

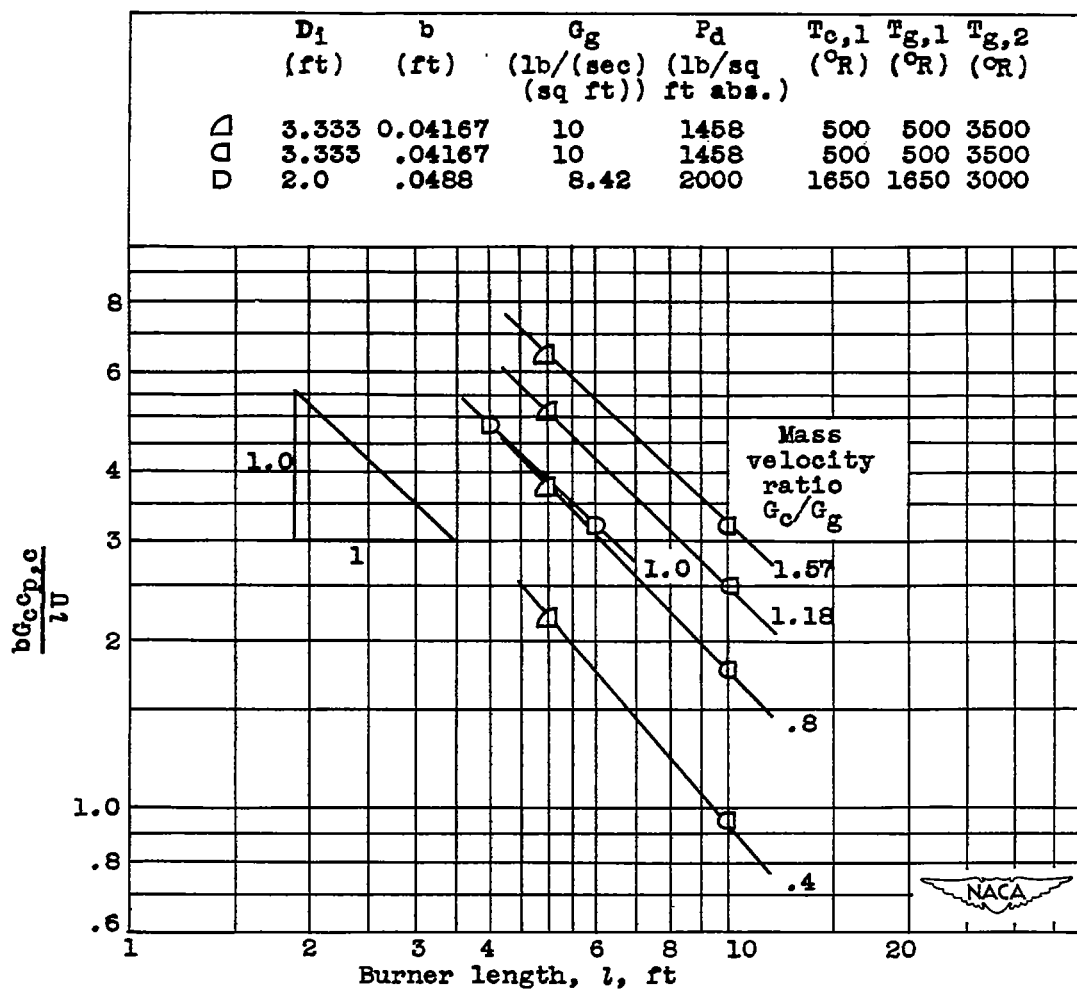
(e) Determination of u .

Figure 6. - Continued. Determination of exponents in empirical equation (19).

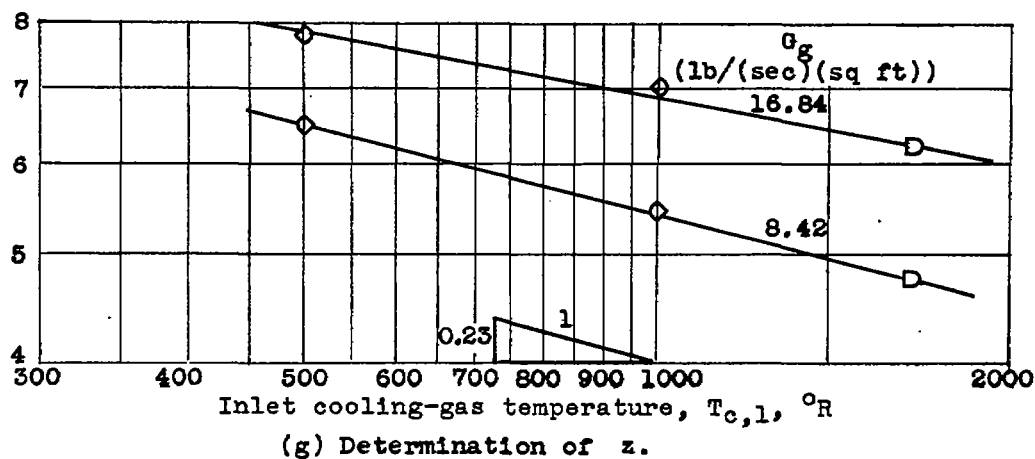
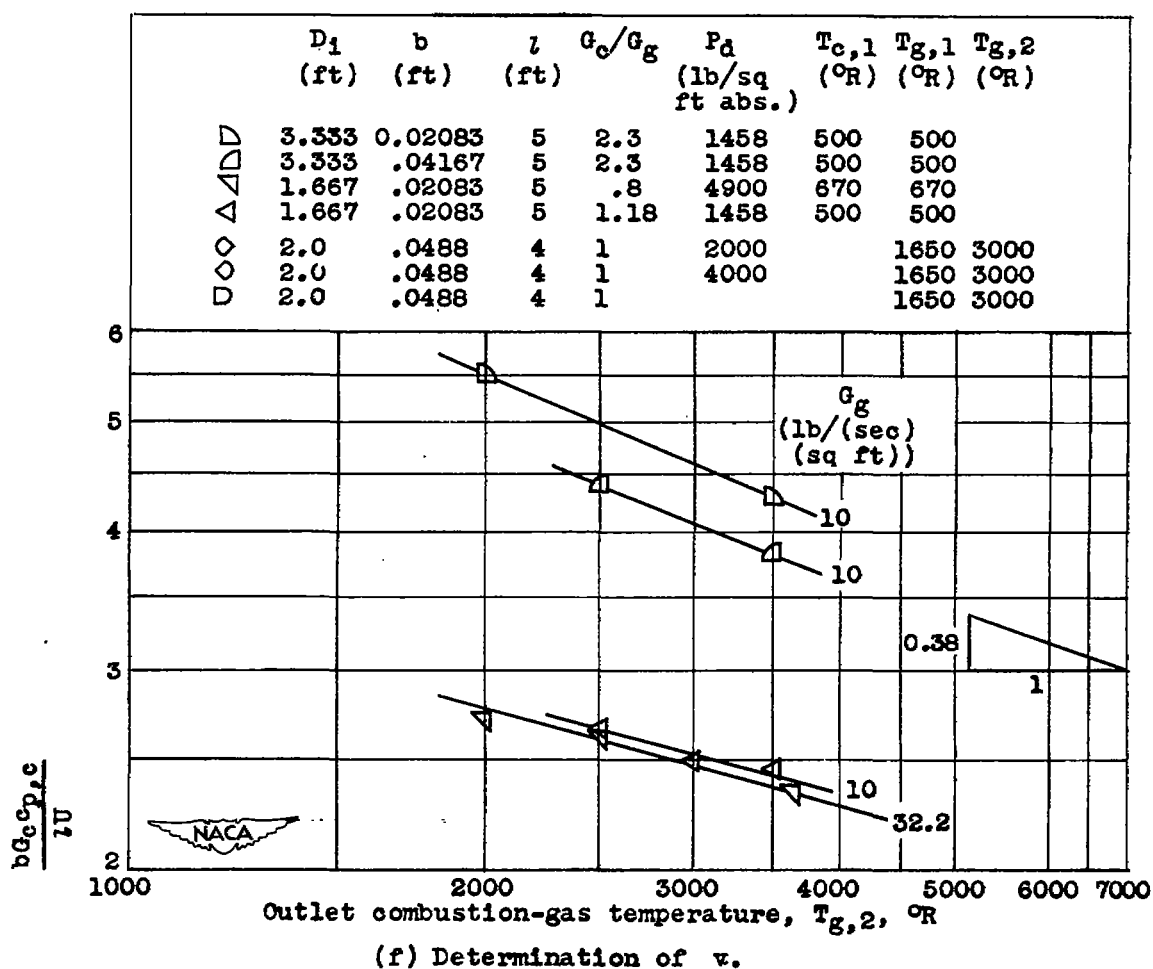


Figure 6. - Concluded. Determination of exponents in empirical equation (19).

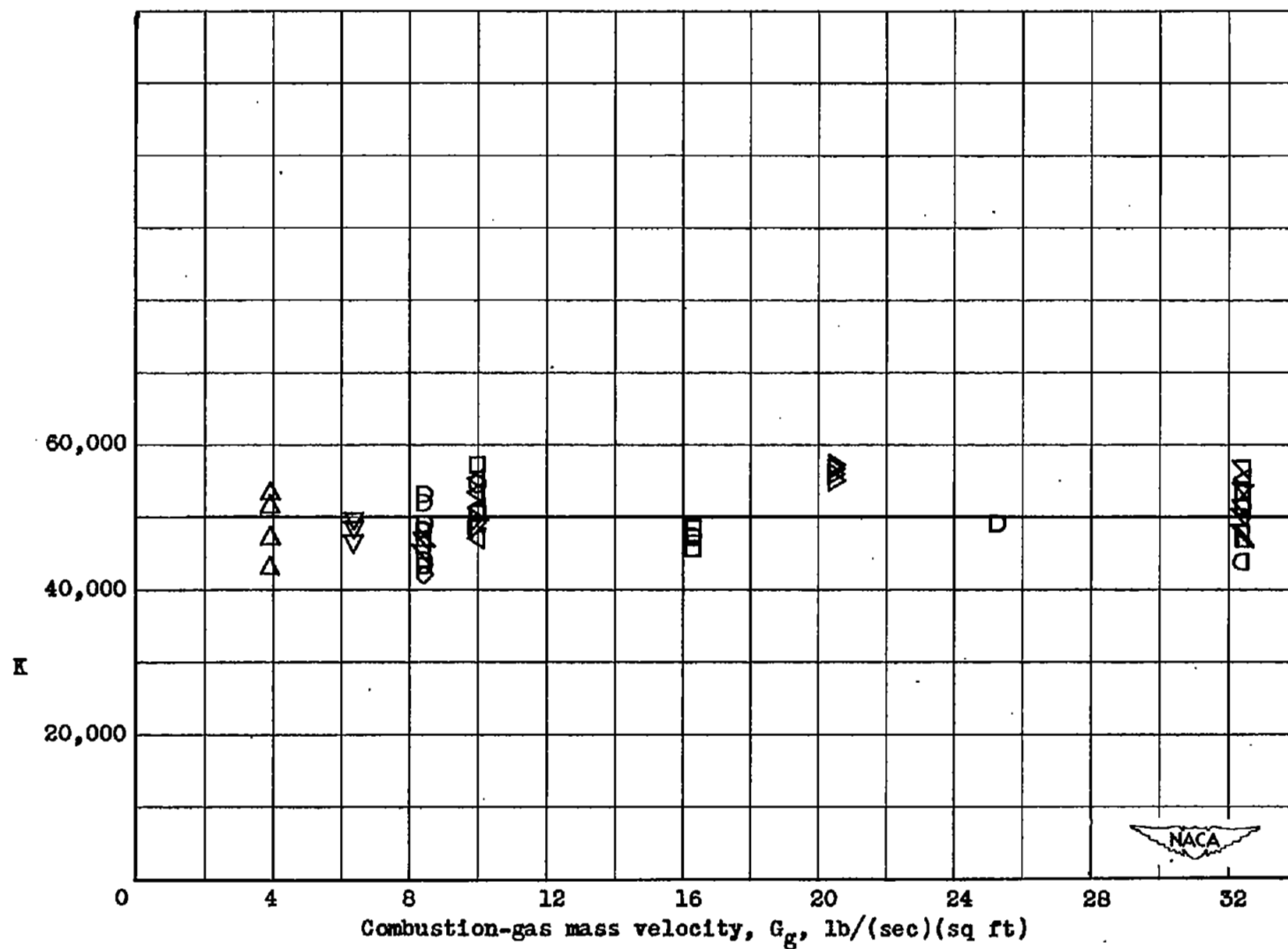
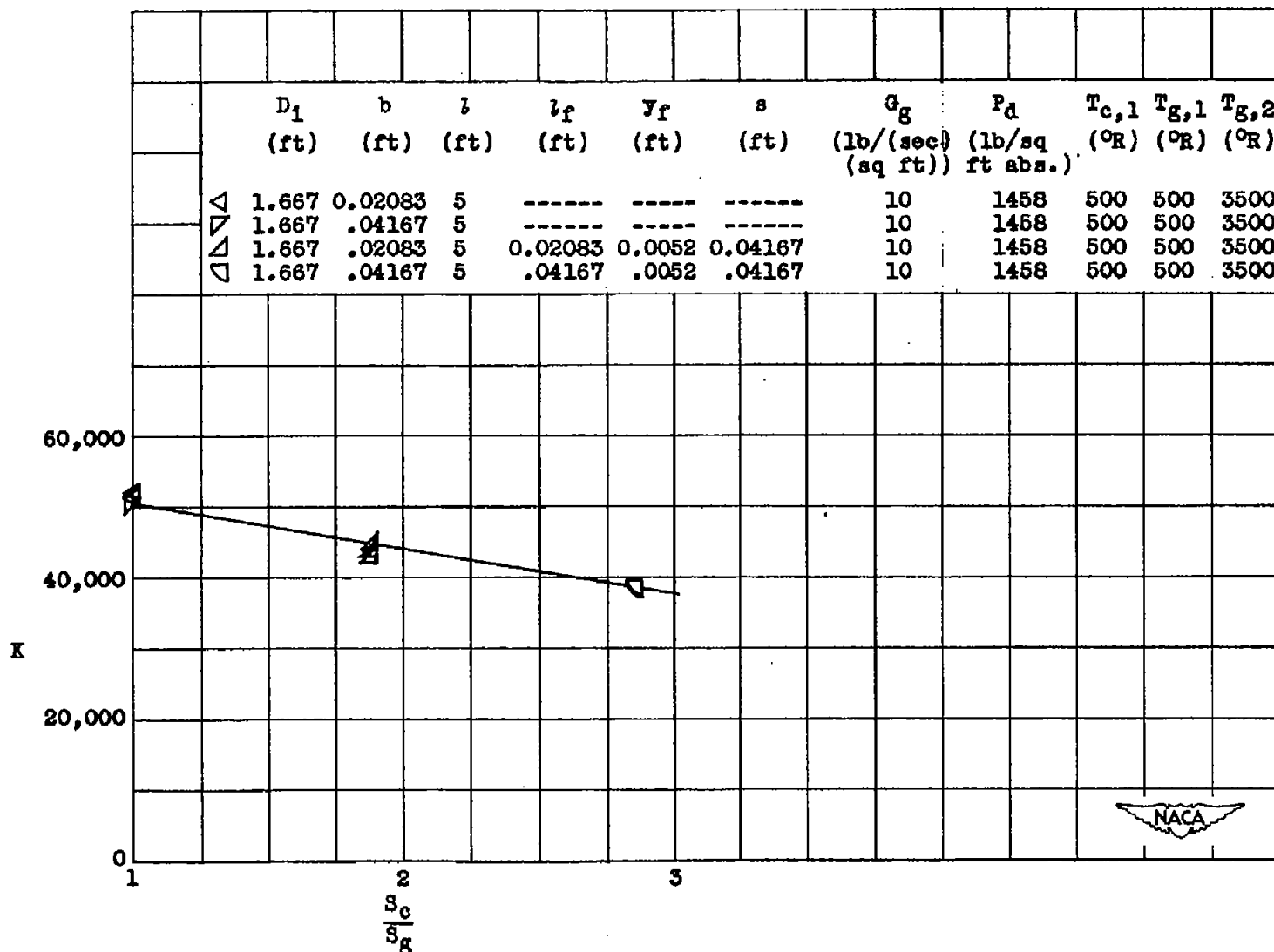


Figure 7. - Determination of mean value of K for annular cooling passage. (See table I for symbols.)

Figure 8. - Effect of Inconel longitudinal fins on K .

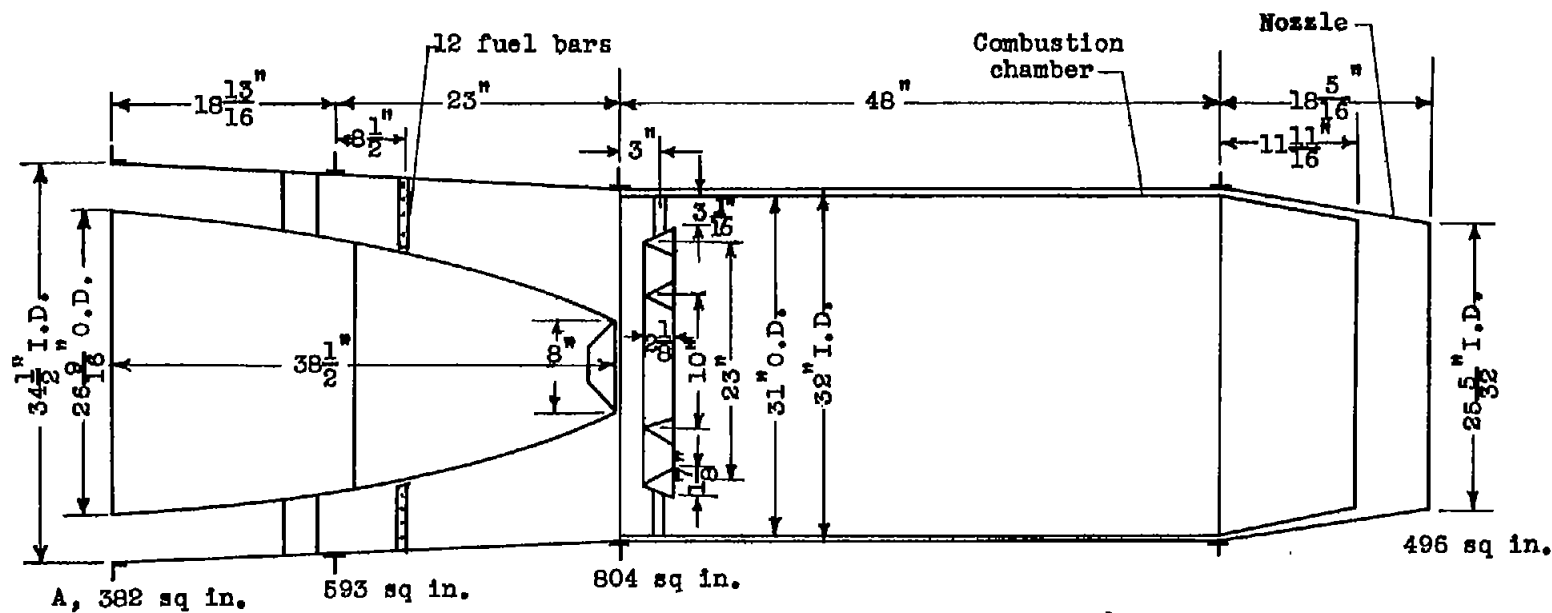


Figure 9. - Experimental tail-pipe burner. Flame-holder blocked area, 240.5 square inches; percentage blocked area, 29.9.

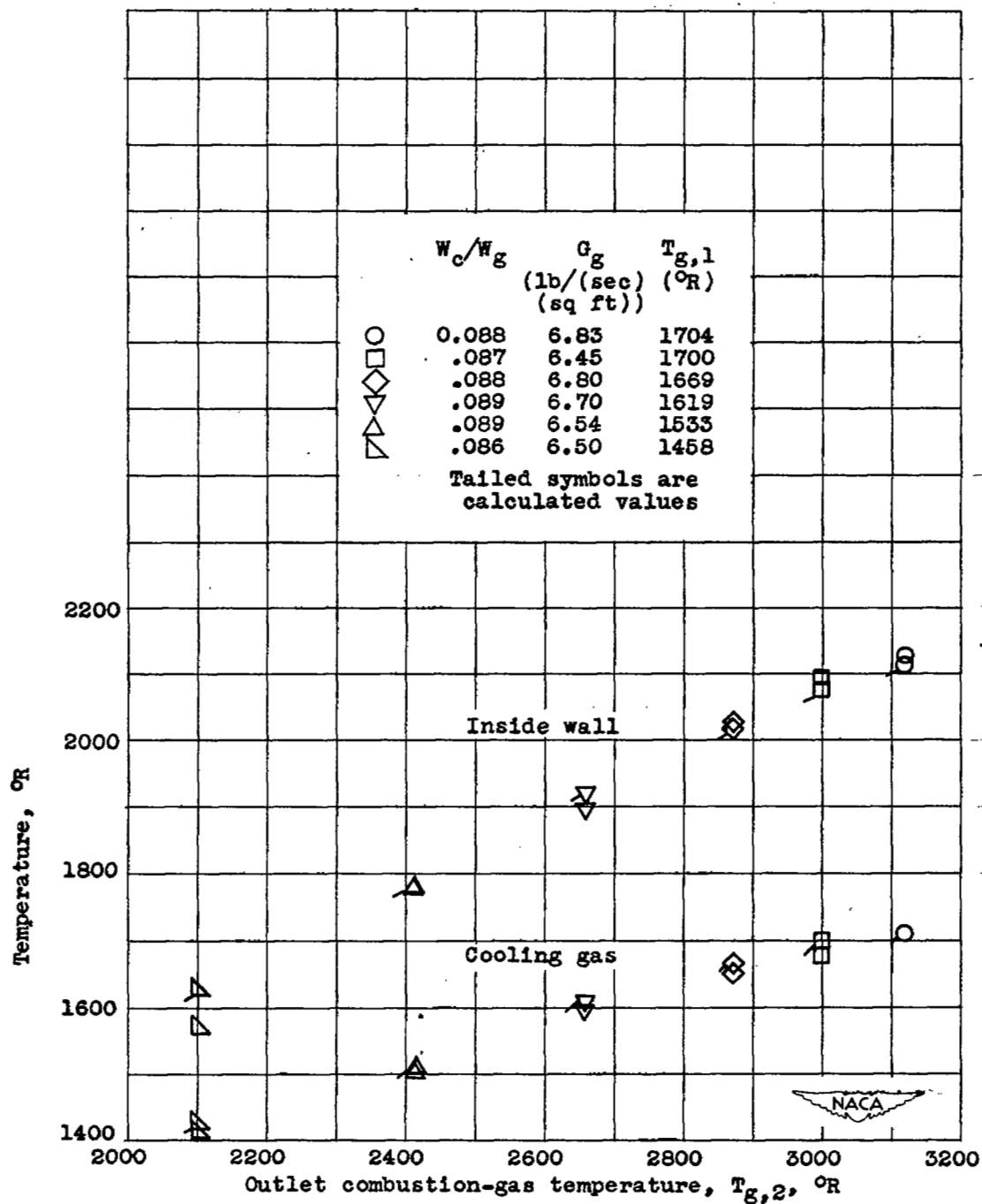


Figure 10. - Variation of inside-wall and cooling-gas temperatures with combustion-gas temperature at 48-inch station of tail-pipe burner shown in figure 9.

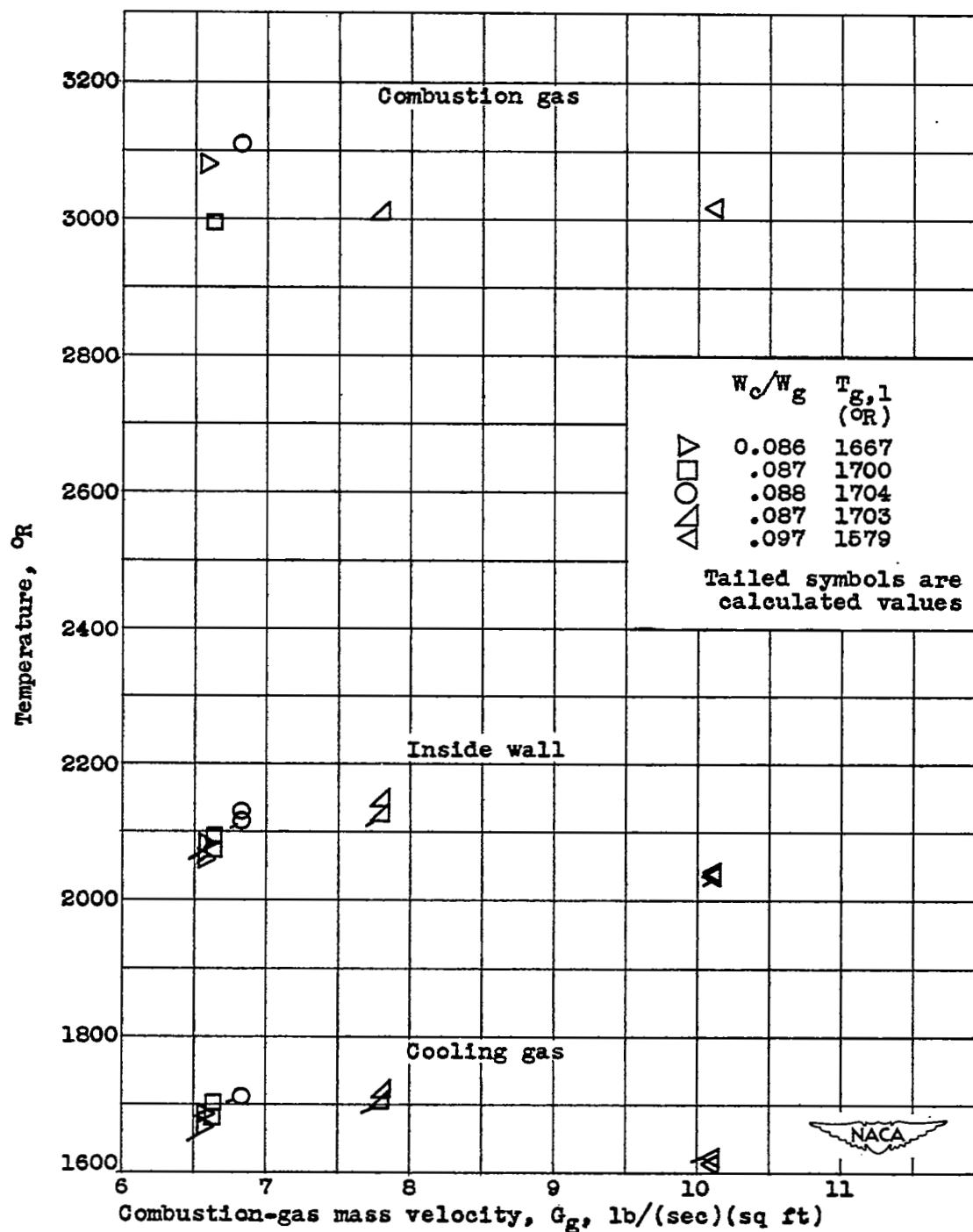


Figure 11. - Comparison of calculated and measured inside-wall and cooling-gas temperatures at 48-inch station of tail-pipe burner shown in figure 9.

NASA Technical Library



3 1176 01434 9089